Self-Assembly of a Water-Soluble Endohedrally Functionalized Coordination Cage Including Polar Guests

Qingqing Sun,[a,b,†] Luis Escobar,[a,b,††,*] Jorn de Jong[a,†††] and Pablo Ballester[a,c,*]

[a] Institute of Chemical Research of Catalonia (ICIQ), The Barcelona Institute of Science and Technology (BIST), Av. Països Catalans 16, 43007 Tarragona (Spain), E-mail: pballester@iciq.es
[b] Universitat Rovira i Virgili (URV), Departament de Química Analítica i Química Orgánica, c/Marcel·lí Domingo 1, 43007 Tarragona (Spain)
[c] ICREA, Passeig Lluís Companys 23, 08010 Barcelona (Spain)
Present addresses:
[†] Yangzhou University, School of Chemistry and Chemical Engineering, Yangzhou, 225002 Jiangsu (China)
[††] Ludwig-Maximilians-Universität München (LMU), Department of Chemistry, Butenandtstrasse 5-13, 81377 München (Germany), E-mail: luis.escobar@cup.lmu.de
[†††] Leiden University, Leiden Institute of Chemistry, Einsteinweg 55, 2333 CC Leiden (The Netherlands)

Supporting Information

Table of Contents

1. General information and instruments....S2
2. Synthesis and characterization data....S2
2.1 Tetra-*α* tetra-pyridyl super aryl-extended calix[4]pyrrole **1b**....S2
2.2 Tetra-*α* tetra-pyridyl super aryl-extended calix[4]pyrrole **2**....S3
2.3 *Bis*-formamide **8**....S5
3. NMR binding studies of tetra-pyridyl SAE-C[4]P **1b** with *mono*-formamide **10**....S6
4. Self-assembly of [**1b**•Pd]$^{2+}$, ^{1}H NMR binding studies of [**1b**•Pd]$^{2+}$ with formamides (**8**, **9** and **10**) and 2D NMR spectra of cage complexes....S8
4.1 Self-assembly of the [**1b**•Pd]$^{2+}$ cage....S8
4.2 NMR binding experiments of [**1b**•Pd]$^{2+}$ with formamides **8**, **9** and **10**....S9
5. Self-assembly of [**2**•Pd]$^{6+}$ using *N*-oxides and formamides (**5**-**10**), 2D NMR spectra of cage complexes and DOSY experiments....S18
5.1 Attempts to self-assemble the [**2**•Pd]$^{6+}$ cage in the absence of guests....S18
5.2 Self-assembly of the [**2**•Pd]$^{6+}$ cage in the presence of pyridine *N*-oxides **5**, **6** and **7**....S18
5.3 Self-assembly of the [**2**•Pd]$^{6+}$ cage in the presence of formamides **8**, **9** and **10**....S26
5.4 Chemical shifts of the *α*-pyridyl protons in the self-assembled Pd(II)-cage complexes....S41
6. Displacement of the included guest in selected cage complexes using the *bis*-*N*-oxide **5** as a competitive binding guest....S42
7. Addition of $(CD_3)_2SO$ to the D_2O solutions of ligand **2**, ligand **2** with *bis*-formamide **8** and selected Pd(II)-cage complexes....S43
8. Energy-minimized structures of the Pd(II)-cage complexes....S47
9. X-ray crystal structures....S48
10. References....S49

1. General information and instruments

Reagents were obtained from commercial suppliers and used without further purification unless otherwise stated. All solvents were commercially obtained and used without further purification except pyrrole which was distilled and freshly used. Dry solvents were taken from a solvent system MB SPS 800. THF, Et_3N, DIPEA and iPr_2NH were dried, distilled and degassed by three freeze-pump-thaw cycles before used in the cross-coupling reactions. Pyridine was dried and distilled before use. Routine ^1H NMR and $^{13}C\{^1H\}$ NMR spectra were recorded on a Bruker Avance 300 (300 MHz for ^1H NMR and 75 MHz for ^{13}C NMR), Bruker Avance 400 (400 MHz for ^1H NMR and 100 MHz for ^{13}C NMR), Bruker Avance 500 (500 MHz for ^1H NMR and 125 MHz for ^{13}C NMR) or Bruker Avance 500 with cryoprobe (500 MHz for ^1H NMR and 125 MHz for ^{13}C NMR). Deuterated solvents used are indicated in the characterization and chemical shifts are given in ppm. Residual solvent peaks were used as reference.[1] All NMR *J* values are given in Hz. COSY, NOESY, ROESY, HMQC and HMBC experiments were recorded to help with the assignment of ^1H and ^{13}C signals. High Resolution Mass Spectra (HRMS) were obtained on a Bruker HPLC-TOF (MicroTOF Focus) and Bruker HPLC-QqTOF (MaXis Impact). Both using ESI as ionization mode. IR spectra were recorded on a Bruker Optics FTIR Alpha spectrometer equipped with a DTGS detector, KBr beamsplitter at 4 cm^{-1} resolution using a one bounce ATR accessory with diamond windows. Melting points were measured on a MP70 Melting Point System Mettler Toledo. Crystal structure determinations were carried out using a Rigaku MicroMax-007HF diffractometer equipped with a PILATUS 200K detector and a Bruker Apex II Duo equipped with an APEX II detector. Both using MoK*α* radiation. Crystal structure solution was achieved using VLD and Patterson methods as implemented in SIR2014 v14.10. Least-squares refinement on F2 using all measured intensities was carried out using the program SHELX-2018/3. Column chromatography was performed with silica gel technical grade (Sigma-Aldrich), pore size 60 Å, 230-400 mesh particle size, 40-63 µm particle size and Thin Layer Chromatography (TLC) analysis on silica gel 60 F254.

2. Synthesis and characterization data

Tetra-*α* 4-iodophenyl-4'-chlorobutyl calix[4]pyrrole **3b**, pyridyl mono-acetylene **4**, tetra-*α* tetra-pyridyl super aryl-extended calix[4]pyrrole **1a** and *bis*-formamide **9** were synthesized following previously reported procedures in the literature.[2,3,4]

2.1 Tetra-*α* tetra-pyridyl super aryl-extended calix[4]pyrrole 1b

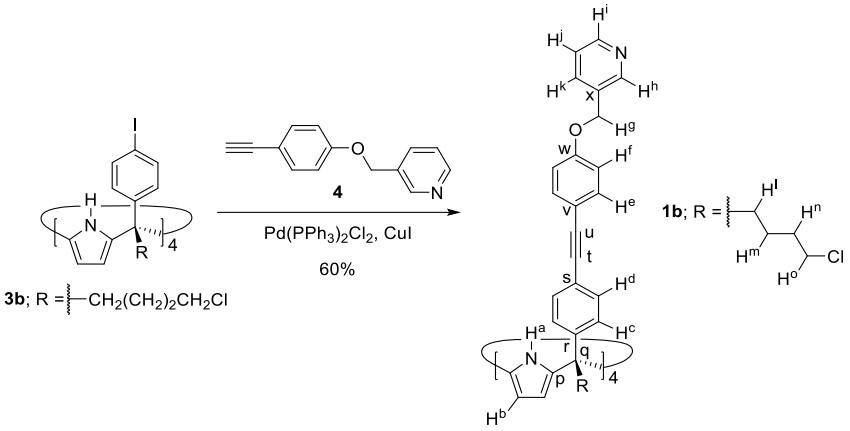

Scheme S1. Synthesis of tetra-pyridyl super aryl-extended calix[4]pyrrole **1b**.

Tetra-*α* 4-iodophenyl-4'-chlorobutyl calix[4]pyrrole **3b** (50 mg, 0.03 mmol, 1 equiv.), $Pd(PPh_3)_2Cl_2$ (2.95 mg, 0.004 mmol, 0.03 equiv.), CuI (1.28 mg, 0.007 mmol, 0.05 equiv.) and 3-((4'-ethynylphenoxy)methyl)pyridine **4** (42.20 mg, 0.20 mmol, 1.5 equiv.) were kept under Argon atmosphere. Dry THF (3.6 mL) and dry diisopropylamine (3.6 mL) were added dropwise. The reaction was stirred at r.t. for 24 h. After that, the crude was concentrated, redissolved in CH_2Cl_2 (10 mL) and washed with brine (2×10 mL) and water (10 mL). The organic layer was dried (Na_2SO_4), filtered and concentrated. The crude was purified by column chromatography on silica gel (3 g, 90:10 → 85:15 CH_2Cl_2/isopropanol) to afford the product as a white solid. The product was further purified by recrystallization from 1:1 CH_2Cl_2/CH_3CN (37 mg, 0.02 mmol, 60% yield). Rf = 0.4 (92:8 CH_2Cl_2/isopropanol). ^1H NMR (500 MHz with cryoprobe, $(CD_3)_2CO$, 298 K): *δ* (ppm) = 8.67 (d, *J* = 1.7 Hz, 4H); 8.53 (dd, *J* = 4.8 Hz, *J* = 1.7 Hz, 4H); 8.48 (s, 4H); 7.82 (ddd, *J* = 7.7 Hz, *J* = 1.7 Hz, *J* = 1.7 Hz, 4H); 7.51-7.49 (m, 8H); 7.42-7.40 (m, 8H); 7.34 (dd, *J* = 7.7 Hz, *J* = 4.8 Hz, 4H); 7.07-7.05 (m, 8H); 7.01-6.99 (m, 8H); 6.05 (d, *J* = 2.7 Hz, 8H); 5.18 (s, 8H); 3.57 (t, *J* = 6.7 Hz, 8H); 2.46-2.43 (m, 8H); 1.79-1.73 (m, 8H); 1.32-1.26 (m, 8H). $^{13}C\{^1H\}$ NMR (125 MHz with cryoprobe, $(CD_3)_2CO$, 298 K): *δ* (ppm) = 159.7; 150.3; 150.1; 147.2; 137.6; 136.1; 133.9; 133.3; 131.9; 130.0; 124.3; 122.8; 116.4; 116.0; 106.4; 90.3; 88.5; 68.4; 49.3; 45.6; 40.9; 33.8; 23.3. MS (MALDI-TOF) *m*/*z*: $[M+H]^+$ Calcd for

$C_{116}H_{101}N_8O_4Cl_4$ 1810.6; Found 1810.7. FTIR *v* (cm^{-1}): 3430; 2950; 1602; 1513; 1428; 1281; 1247; 1018; 829; 771. M.p. > 220ºC (decompose).

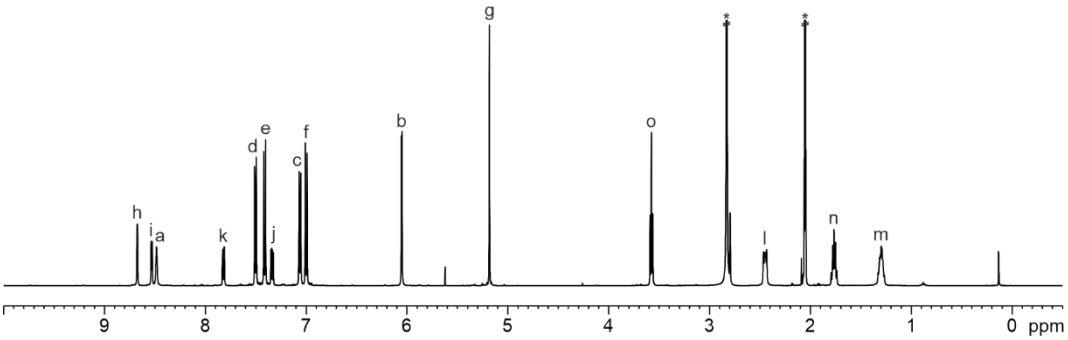

Figure S1. ^1H NMR (500 MHz with cryoprobe, $(CD_3)_2CO$, 298 K) spectrum of compound **1b**. See Scheme S1 for proton assignment. *Residual solvent peaks.

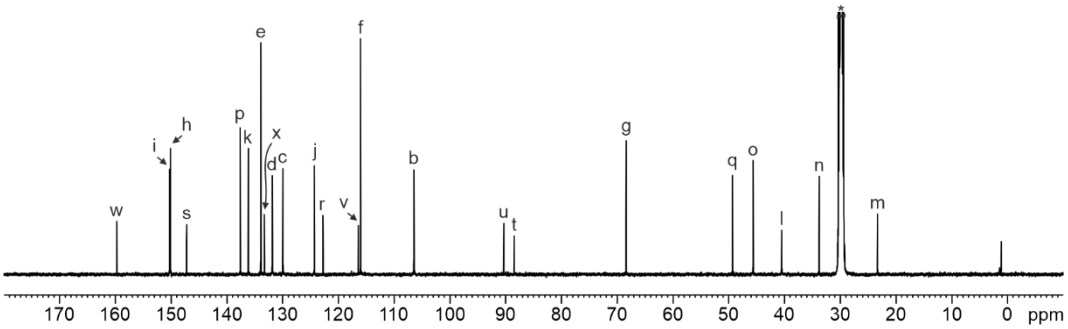

Figure S2. $^{13}C\{^1H\}$ NMR (125 MHz with cryoprobe, $(CD_3)_2CO$, 298 K) spectrum of compound **1b**. See Scheme S1 for carbon assignment. *Residual solvent peak.

2.2 Tetra-*α* tetra-pyridyl super aryl-extended calix[4]pyrrole 2

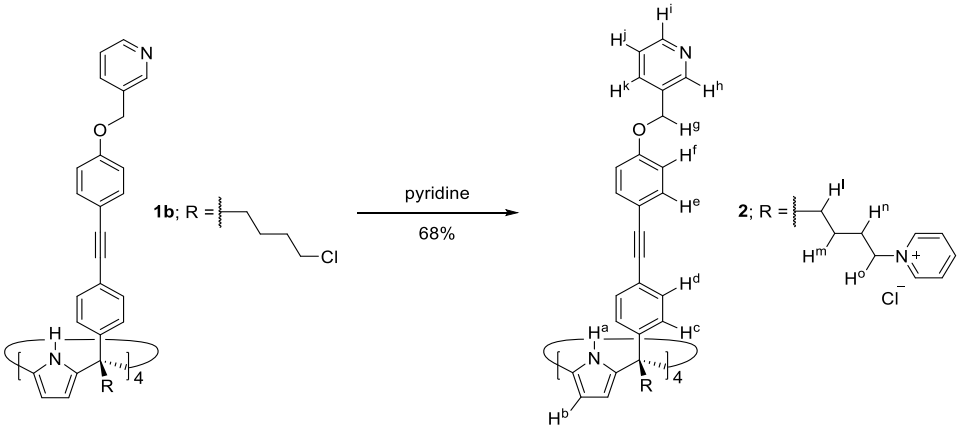

Scheme S2. Synthesis of tetra-pyridyl super aryl-extended calix[4]pyrrole **2**.

Tetra-pyridyl super aryl-extended calix[4]pyrrole **1b** (20 mg, 0.011 mmol, 1 equiv.) was added to a dry-oven schlenk flask and kept under Argon atmosphere. Freshly distilled and dry pyridine (2.2 mL) was added and the reaction was stirred at 110ºC overnight. After that, the reaction was stopped and allowed to reach r.t. The crude was concentrated, and acetone (3 mL) was added and sonicated. The crude was filtered and washed with acetone (3 mL), CH_2Cl_2 (2×3 mL) and hexane (2×3 mL) affording the product as a pale brown solid (16 mg, 0.007 mmol, 68% yield). ^1H NMR (500 MHz with cryoprobe, CD_3OD, 333 K): *δ* (ppm) = 8.87-8.86 (m, 8H); 8.56 (s, 4H); 8.54-8.52 (m, 4H); 8.46 (d, *J* = 4.8 Hz, 4H); 8.03-8.01 (m, 8H); 7.86 (d, *J* = 7.8 Hz, 4H); 7.40-7.36 (m, 20 H); 7.02-7.00 (m, 8H); 6.96-6.94 (m, 8H); 5.95 (s, 8H); 5.14 (s, 8H); 4.56 (t, *J* = 7.4 Hz, 8H); 2.49-2.46 (m, 8H); 2.01-1.95 (m, 8H); 1.30-1.24 (m, 8H). $^{13}C\{^1H\}$ NMR (125 MHz with cryoprobe, CD_3OD, 333 K): *δ* (ppm) = 160.1; 149.8; 149.4; 146.9; 145.8; 137.8; 137.3; 134.7; 134.2; 131.9; 129.8; 129.5; 125.1; 123.4; 117.3; 116.4; 106.8; 68.8; 62.9; 40.3; 32.7; 23.1 (the signal/noise ratio of some carbons was too low for an unequivocal assignment). HRMS (ESI-TOF) *m*/*z*: $[M-4Cl]^{4+}$

Calcd for $C_{136}H_{120}N_{12}O_4$ 496.2383; Found 496.2398. FTIR *v* (cm^{-1}): 3363; 3190; 2942; 1600; 1512; 1485; 1241; 1173; 1017; 770. M.p. > 260ºC (decompose).

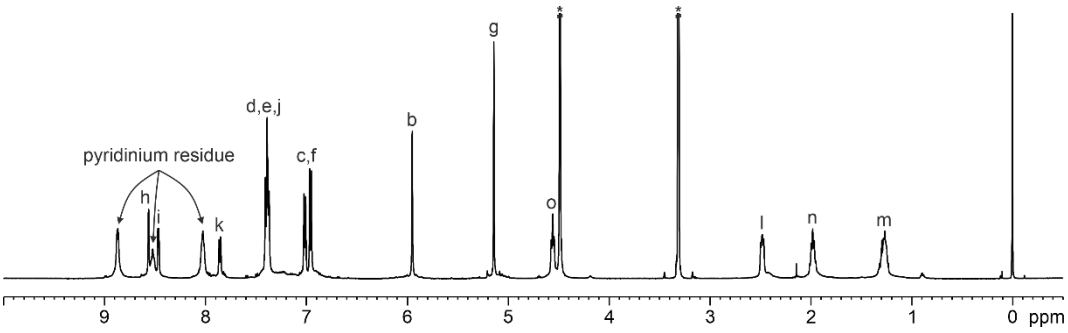

Figure S3. ^{1}H NMR (500 MHz with cryoprobe, CD_3OD, 333 K) spectrum of compound $\mathbf{2}^{4+}$. See Scheme S2 for proton assignment. *Residual solvent peaks.

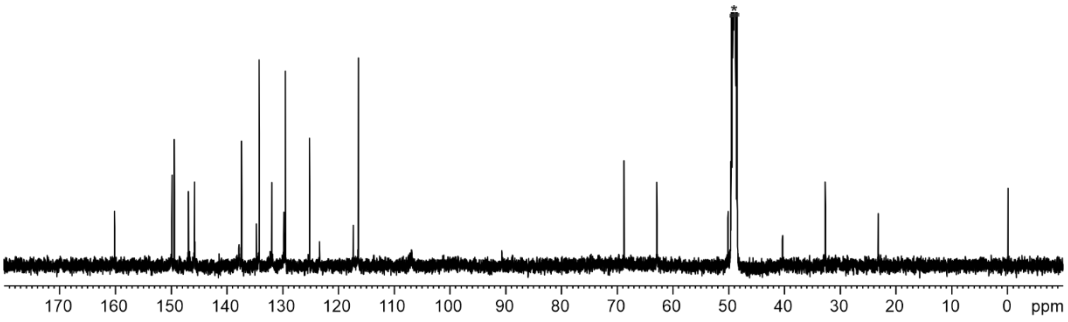

Figure S4. $^{13}C\{^{1}H\}$ NMR (125 MHz with cryoprobe, CD_3OD, 333 K) spectrum of compound $\mathbf{2}^{4+}$. *Residual solvent peak.

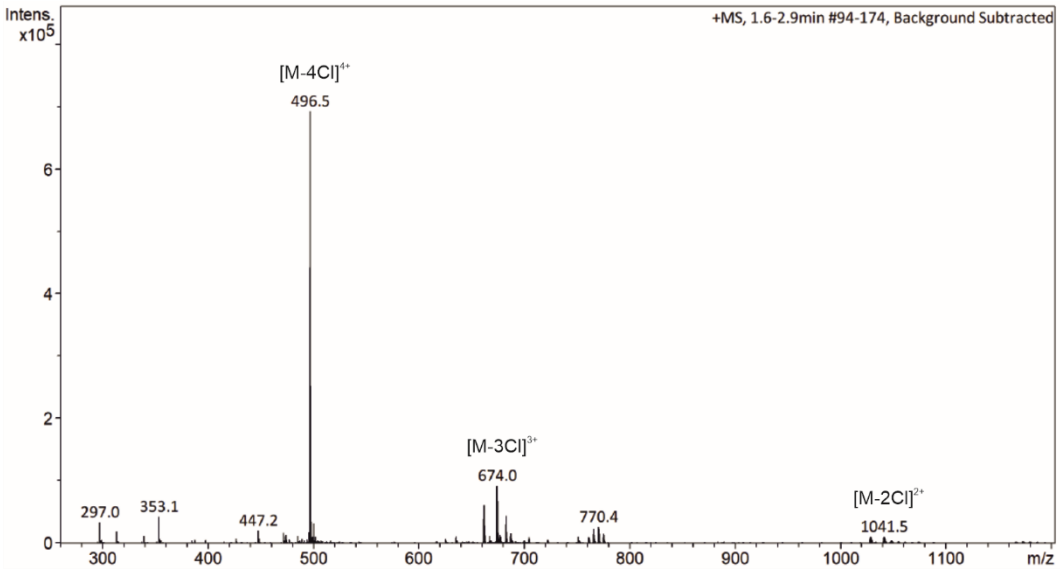

Figure S5. MS spectrum of compound **2**.

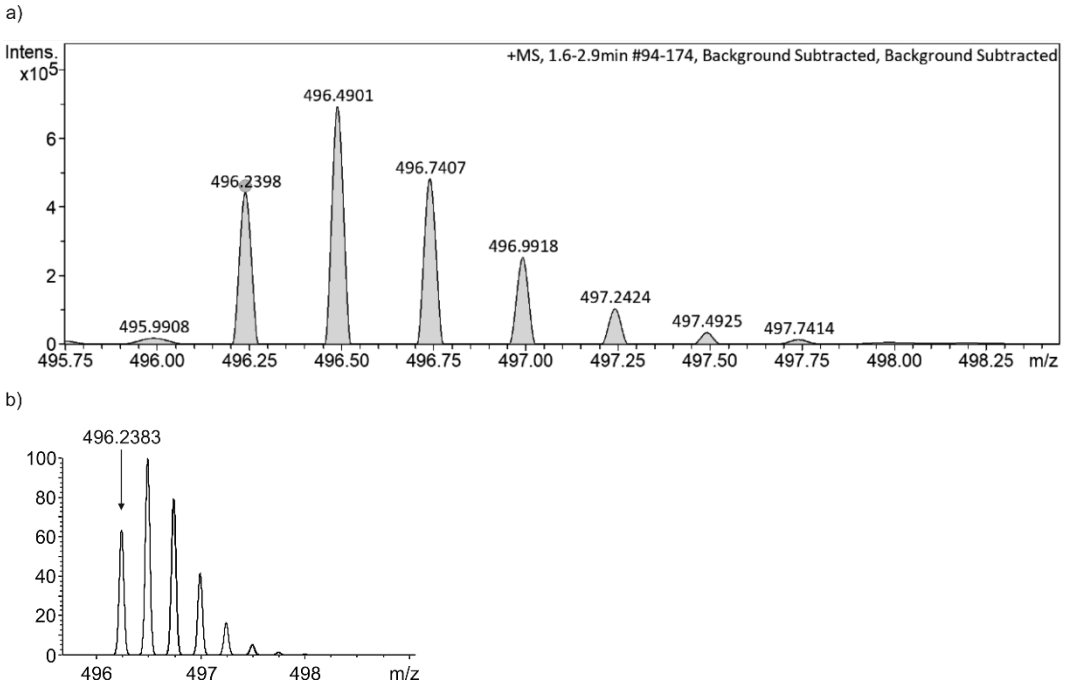

Figure S6. Selected region of the MS spectrum of compound **2**: a) experimental and b) theoretical isotopic distributions of $[M\text{-}4Cl]^{4+}$. The exact mass for the mono-isotopic peak in a) and b) is indicated.

2.3 *Bis*-formamide 8

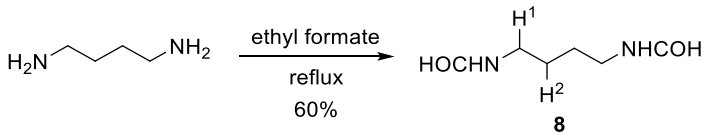

Scheme S3. Synthesis of *bis*-formamide **8**.

1,4-*Bis*-aminobutane (0.10 g, 1.12 mmol, 1 equiv.) was dissolved in ethyl formate (0.50 M of reactant). The reaction was heated under reflux conditions overnight. After that, the crude was concentrated under reduced pressure. The crude was purified by silica gel column chromatography (acetone) to afford the product as a white solid (0.10 g, 0.67 mmol, 60% yield). ^{1}H NMR (400 MHz, D_2O, 298 K): δ (ppm) = 8.04 (s, 1.7H); 7.98 (s, 0.3H); 3.28-3.24 (m, 4H); 1.59-1.55 (m, 4H). $^{13}C\{^{1}H\}$ NMR (100 MHz, D_2O, 298 K): δ (ppm) = 164.3; 37.7; 25.8 (*trans*,*trans*-isomer, major). HRMS (ESI-TOF) *m*/*z*: $[M+Na]^+$ Calcd for $C_6H_{12}N_2NaO_2$ 167.0791; Found 167.0783.

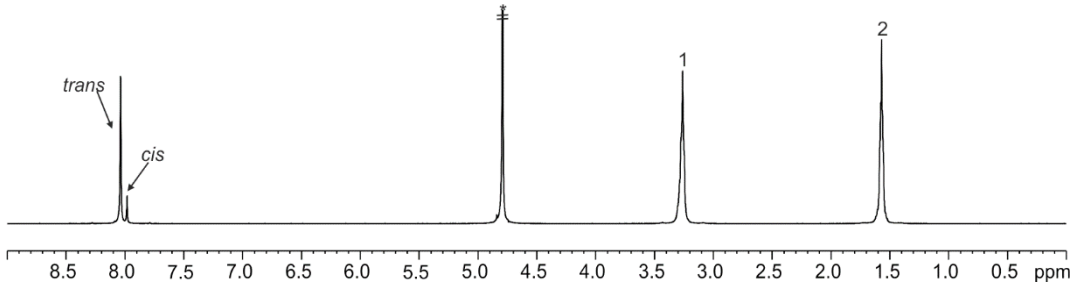

Figure S7. ^{1}H NMR (400 MHz, D_2O, 298 K) spectrum of compound **8**. See Scheme S3 for proton assignment. *Residual solvent peak.

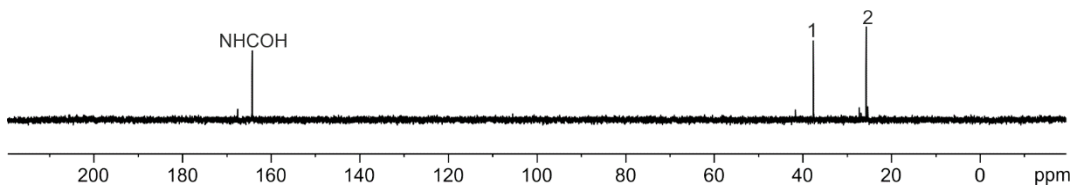

Figure S8. $^{13}C\{^{1}H\}$ NMR (100 MHz, D_2O, 298 K) spectrum of compound **8**. See Scheme S3 for carbon assignment.

3. NMR binding studies of tetra-pyridyl SAE-C[4]P 1b with *mono*-formamide 10

A solution of the tetra-pyridyl SAE-C[4]P **1b** (1 mM) was prepared in $CDCl_3$ or in 2:1 $CDCl_3/CD_3CN$ solution. Subsequently, 0.5 mL of the solution were placed in an NMR tube. A solution of the guest **10** was prepared at 20-30-fold higher concentration using the host's solution ([G] = 20-30 mM and [H] = 1 mM). Immediately, the 0.5 mL of the tetra-pyridyl's solution was titrated by manually injecting incremental amounts of the guest's solution using a micro syringe. A ^{1}H NMR spectrum of the mixture was acquired after each injection and vigorous hand shaking of the NMR tube for few seconds.

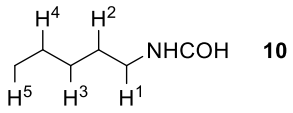

10

Figure S9. Line-drawing structure of formamide **10**.

^{1}H NMR titration spectra in $CDCl_3$

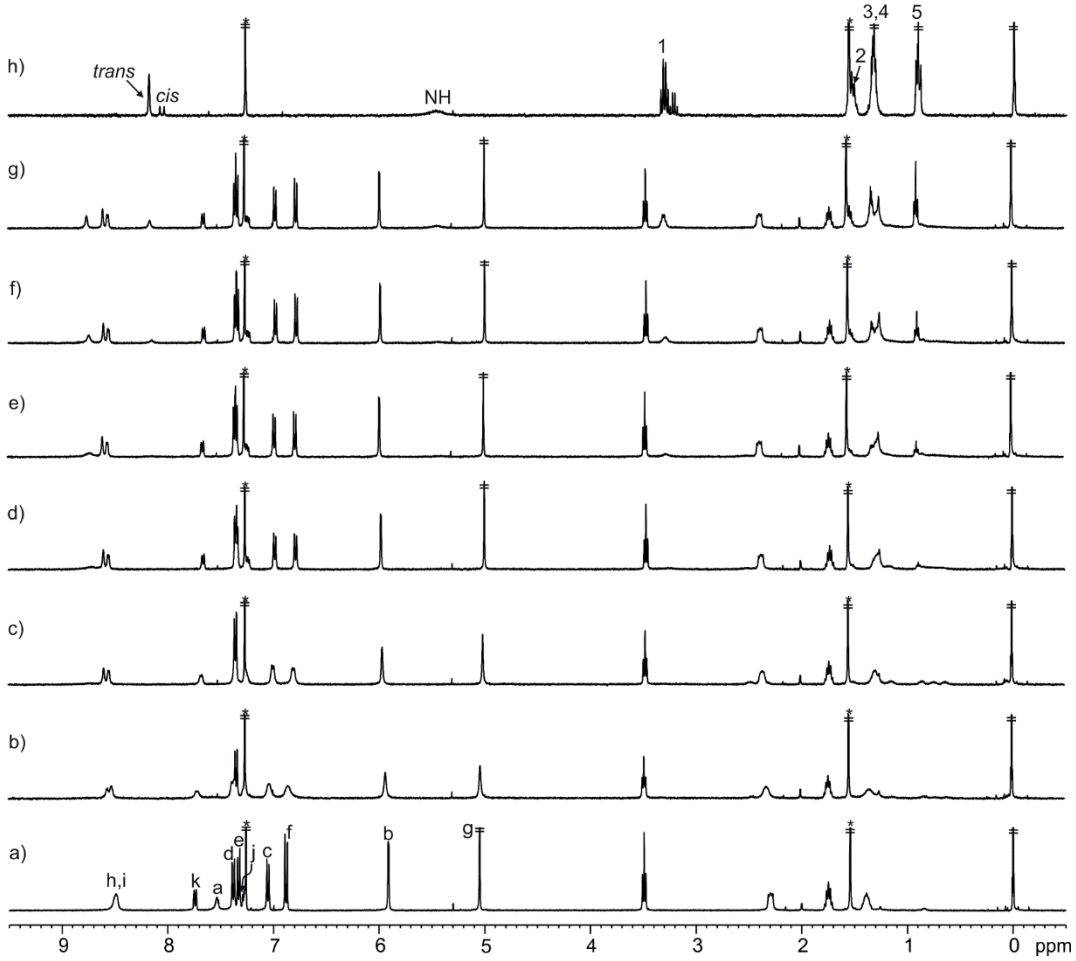

Figure S10. Selected ^{1}H NMR (400 MHz, $CDCl_3$, 298 K) spectra of the titration of **1b** with **10**: a) 0; b) 0.5; c) 1; d) 1.5; e) 2; f) 3 and g) 5 equiv.; h) **10**. See Scheme S1 and Figure S9 for proton assignments. *Residual solvent peaks.

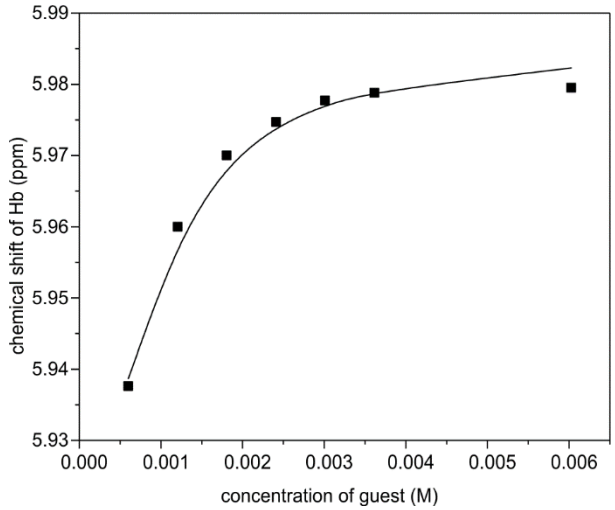

Figure S11. Fit of the NMR titration data (proton signal H^b of **1b**) to a theoretical 1:1 binding model. The fit returned an apparent binding constant value K_{app} (**10**⊂**1b**) = 3×10^3 M^{-1}.

^{1}H NMR titration spectra in 2:1 $CDCl_3/CD_3CN$

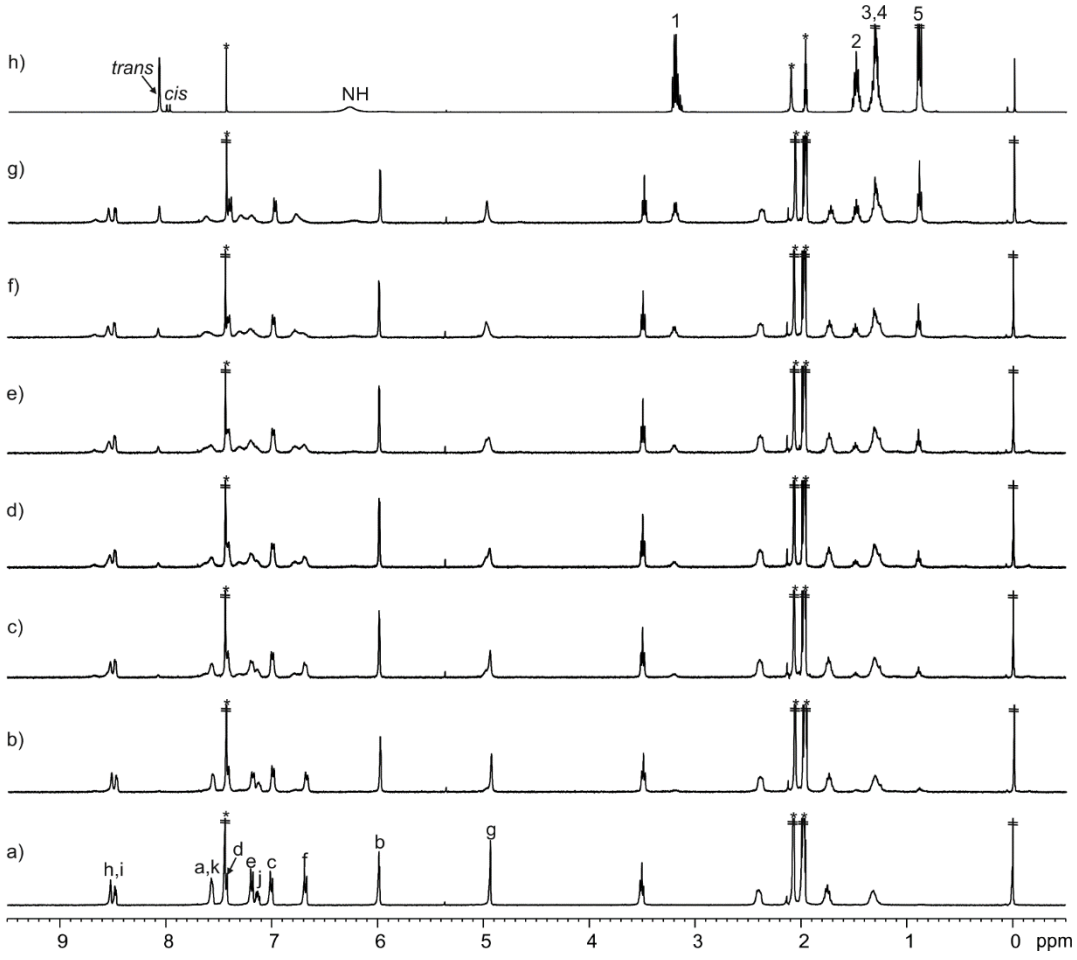

Figure S12. Selected ^{1}H NMR (400 MHz, 2:1 $CDCl_3/CD_3CN$, 298 K) spectra of the titration of **1b** with **10**: a) 0; b) 0.5; c) 1; d) 1.5; e) 2; f) 3 and g) 5 equiv.; h) **10**. See Scheme S1 and Figure S9 for proton assignments. *Residual solvent peaks.

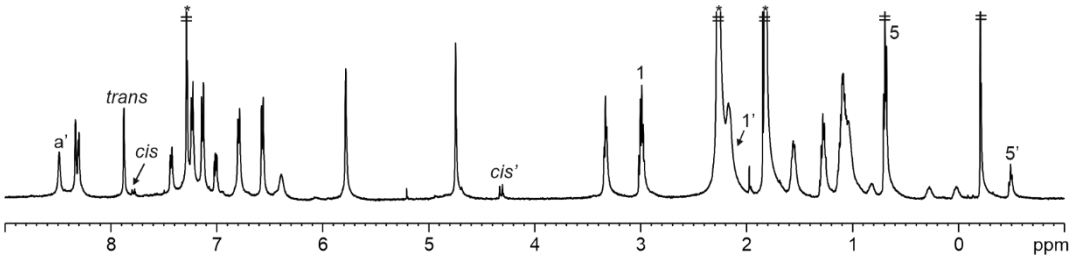

Figure S13. ^{1}H NMR (500 MHz, 2:1 $CDCl_3/CD_3CN$, 233 K) spectrum of **1b** with 5 equiv. of **10**. See Scheme S1 and Figure S9 for proton assignments. *Residual solvent peaks.

Based on the relative integral values of the proton signals of the free and bound components in the ^{1}H NMR spectrum at 233 K, we estimated an apparent binding constant value K_{app} (**10**⊂**1b**) ~ 7 × 10^2 M^{-1}.

4. Self-assembly of [1b•Pd]$^{2+}$, ^{1}H NMR binding studies of [1b•Pd]$^{2+}$ with formamides (8, 9 and 10) and 2D NMR spectra of cage complexes

A solution of the tetra-pyridyl SAE-C[4]P **1b** (1 mM) and 1,3,5-trimethoxybenzene (internal standard, 1 mM) was prepared in 2:1 $CDCl_3/CD_3CN$ solution. Subsequently, 0.5 mL of the solution were placed in an NMR tube. A solution of $[Pd(CH_3CN)_4](BF_4)_2$ was prepared in 2:1 $CDCl_3/CD_3CN$ at higher concentration (5-7 mM). Immediately, the 0.5 mL of the tetra-pyridyl's solution was titrated by manually injecting incremental amounts of the Pd(II) solution using a micro syringe. A ^{1}H NMR spectrum of the mixture was acquired after each injection and vigorous hand shaking of the NMR tube for few seconds. The solution contained in the NMR tube was thermally equilibrated at 40ºC for 24 h in an oil bath. After that, a solution of the guest (**8**, **9** and **10**) was prepared in 2:1 $CDCl_3/CD_3CN$ at higher concentration (20-40 mM). The cage's solution was titrated by manually injecting incremental amounts of the guest's solution using a micro syringe. A ^{1}H NMR spectrum of the mixture was acquired after each injection and vigorous hand shaking of the NMR tube for few seconds.

4.1 Self-assembly of the [1b•Pd]$^{2+}$ cage

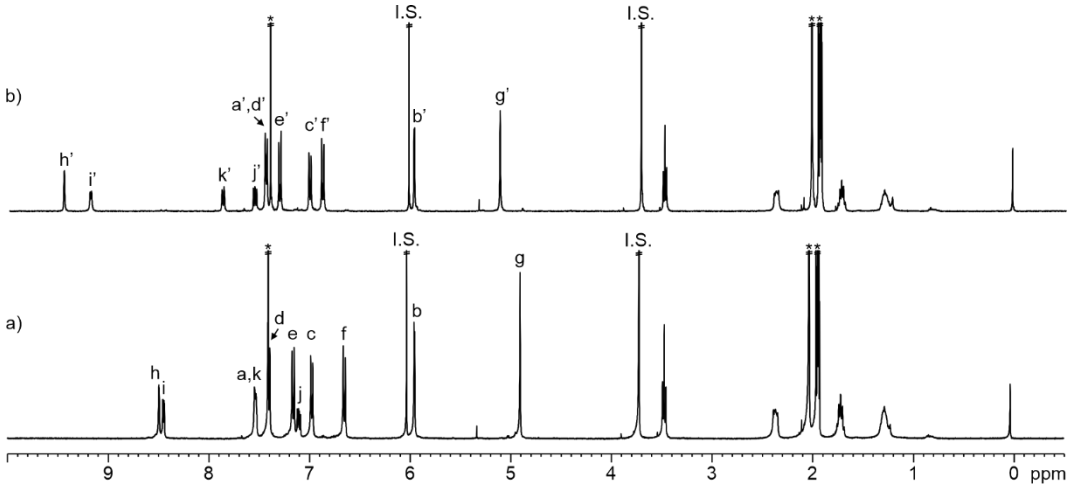

Figure S14. ^{1}H NMR (400 MHz, 2:1 $CDCl_3/CD_3CN$, 298 K) spectra: a) **1b**; addition of $[Pd(CH_3CN)_4](BF_4)_2$ to **1b** followed by thermal equilibration (40ºC for 24 h): b) *ca.* 1 equiv. Primed labels correspond to proton signals of [**1b**•Pd]$^{2+}$. The [**1b**•Pd]$^{2+}$ cage was assembled in 90% extent. See Scheme S1 for proton assignment. 1,3,5-Trimethoxybenzene (I.S.). *Residual solvent peaks.

4.2 NMR binding experiments of [1b•Pd]$^{2+}$ with formamides 8, 9 and 10

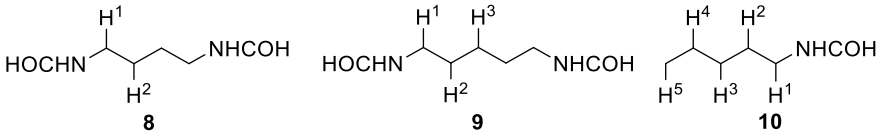

Figure S15. Line-drawing structures of formamides **8**, **9** and **10**.

Bis-formamide **8**

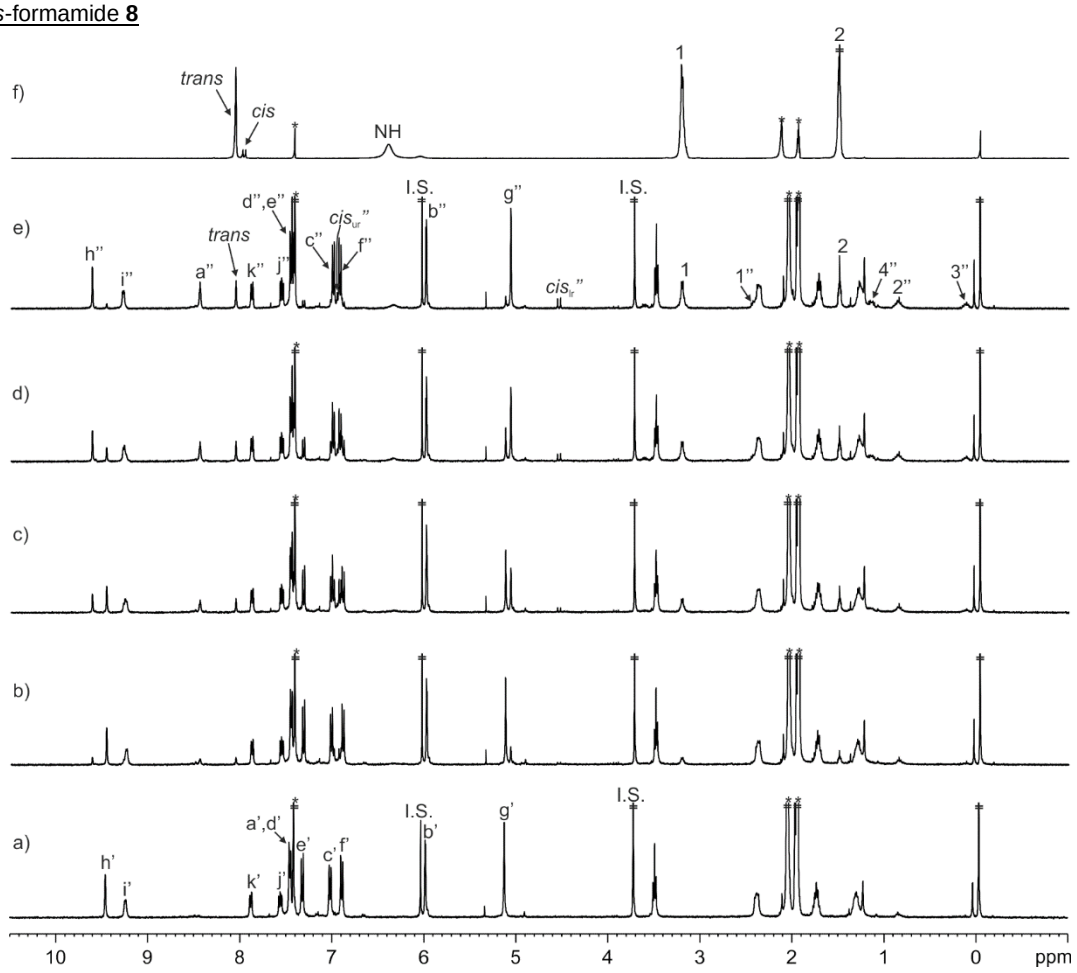

Figure S16. ^{1}H NMR (400 MHz, 2:1 $CDCl_3/CD_3CN$, 298 K) spectra of the titration of [**1b**•Pd]$^{2+}$ with **8**: a) 0; b) 0.5; c) 1; d) 1.5 and e) 2 equiv.; f) **8**. Primed labels correspond to proton signals of [**1b**•Pd]$^{2+}$. Doubly primed labels correspond to proton signals of *cis,cis*-**8**⊂[**1b**•Pd]$^{2+}$. See Scheme S1 and Figure S22 for proton assignments. 1,3,5-Trimethoxybenzene (I.S.). *Residual solvent peaks.

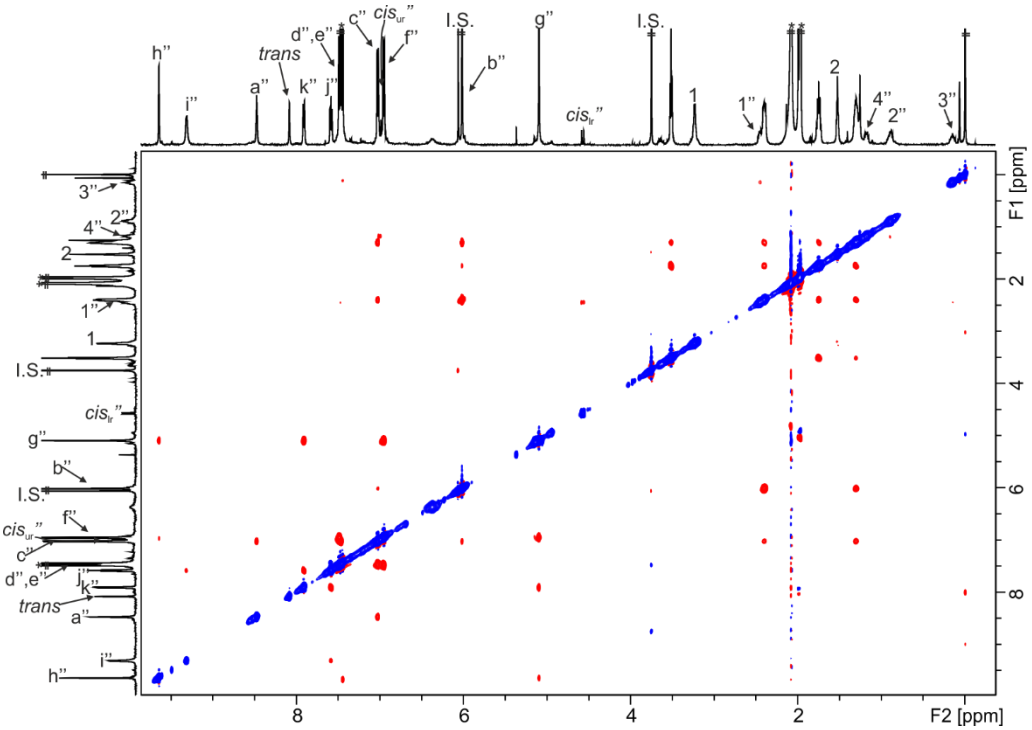

Figure S17. ^{1}H-^{1}H ROESY NMR (500 MHz with cryoprobe, 2:1 $CDCl_3/CD_3CN$, 298 K, spin lock = 0.3 s) spectrum of [**1b**•Pd]$^{2+}$ with 2 equiv. of **8**. See Figure S22 for proton assignment. *Residual solvent peaks.

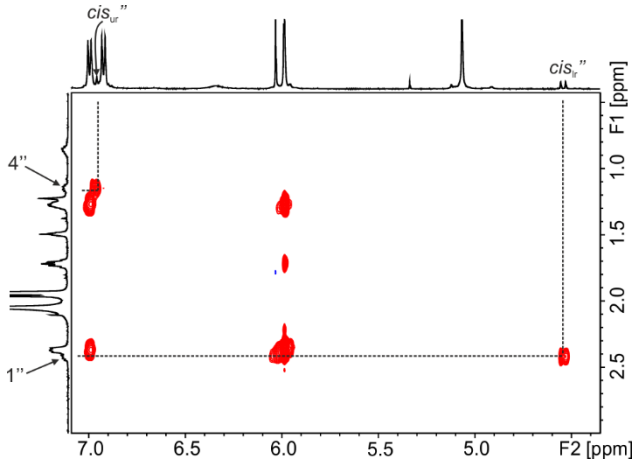

Figure S18. Selected region of the ^{1}H-^{1}H ROESY NMR (500 MHz with cryoprobe, 2:1 $CDCl_3/CD_3CN$, 298 K, spin lock = 0.3 s) spectrum of [**1b**•Pd]$^{2+}$ with 2 equiv. of **8**. The ROESY cross-peaks between 1'' and 4'' with the signals at 4.54 and 6.96 ppm, respectively, are highlighted. The observed cross-peaks confirm that the two formamide groups of bound **8** adopt a *cis*-conformation. See Figure S22 for proton assignment.

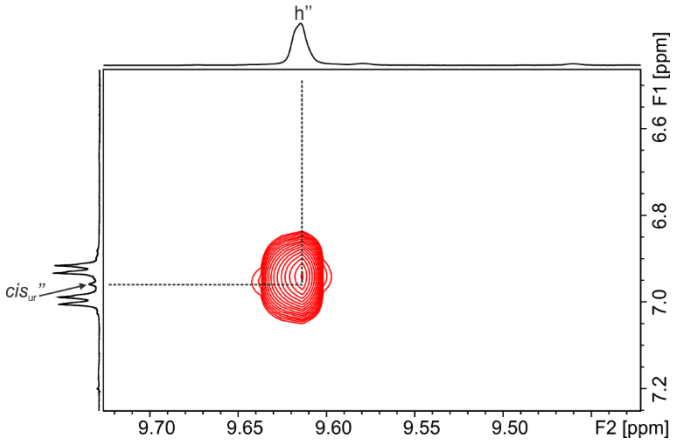

Figure S19. Selected region of the ^{1}H-^{1}H ROESY NMR (500 MHz with cryoprobe, 2:1 $CDCl_3/CD_3CN$, 298 K, spin lock = 0.3 s) spectrum of [**1b**•Pd]$^{2+}$ with 2 equiv. of **8**. The ROESY cross-peak between h'' and *cis*$_{ur}$'' is highlighted. The observed cross-peak indicates that one of the formamide groups of bound *cis*,*cis*-**8** is located in the binding site defined by the inwardly-directed *α*-pyridyl protons. See Scheme S1 and Figure S22 for proton assignments.

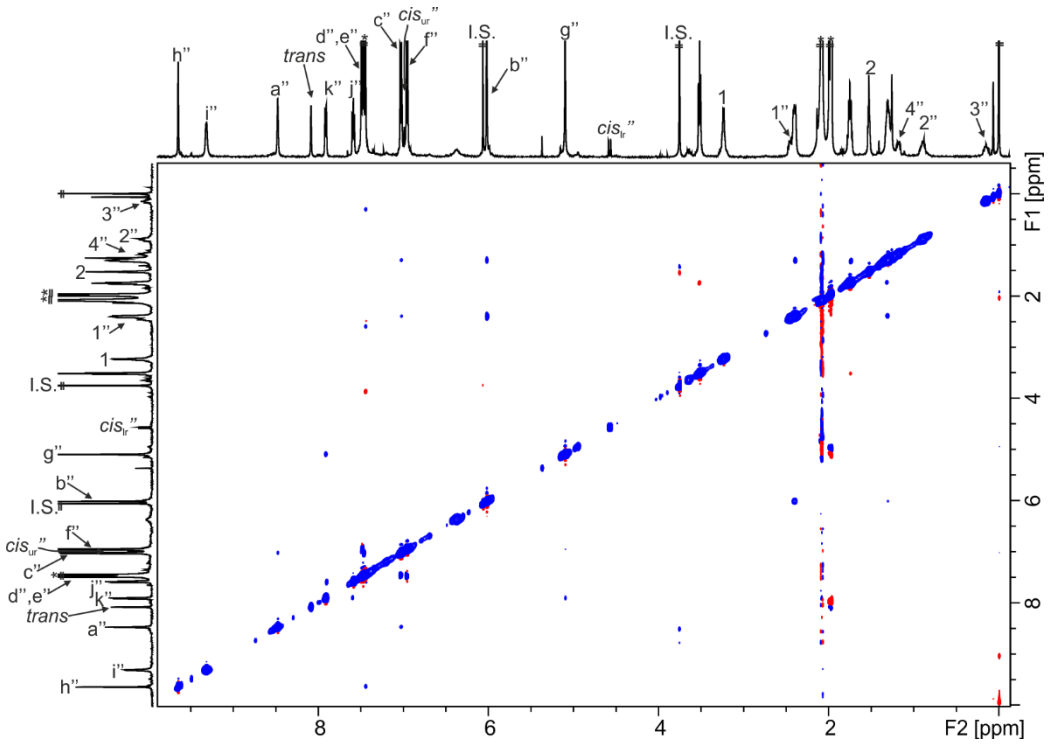

Figure S20. ^{1}H-^{1}H EXSY NMR (500 MHz with cryoprobe, 2:1 $CDCl_3/CD_3CN$, 298 K, mixing time = 0.3 s) spectrum of [**1b**•Pd]$^{2+}$ with 2 equiv. of **8**. See Figure S15 and Figure S22 for proton assignments. *Residual solvent peaks.

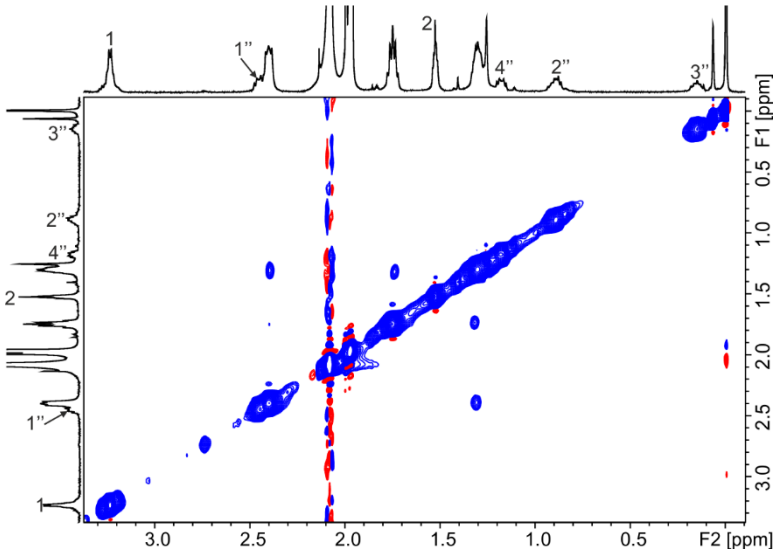

Figure S21. Selected region of the ^{1}H-^{1}H EXSY NMR (500 MHz with cryoprobe, 2:1 $CDCl_3/CD_3CN$, 298 K, mixing time = 0.3 s) spectrum of [**1b**•Pd]$^{2+}$ with 2 equiv. of **8**. See Figure S15 and Figure S22 for proton assignments.

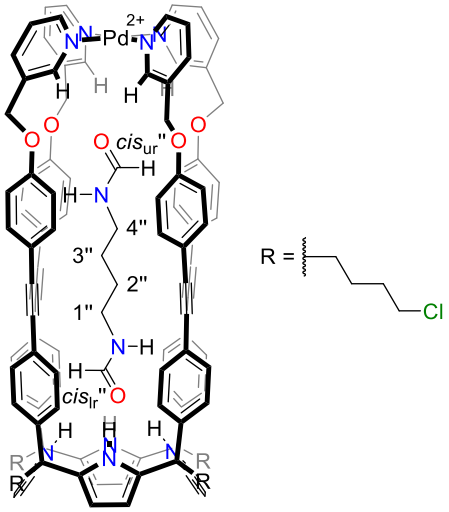

Figure S22. Line-drawing structure of the *cis*,*cis*-**8**⊂[**1b**•Pd]$^{2+}$ cage complex.

Table S1. Experimental chemical shifts of free (δ_{free}) and bound (δ_{bound}) *bis*-formamide **8** and complexation-induced shifts ($\Delta\delta$).

Signal	δ_{free} (ppm)	Signal	δ_{bound} (ppm)	$\Delta\delta$ (ppm)
trans	8.08	-	-	-
cis	7.99	cis_{lr}''	4.54	-3.45
-	-	cis_{ur}''	6.96	-1.03
1	3.23	1''	2.45	-0.78
2	1.53	2''	0.89	-0.64
-	-	3''	0.15	-1.38
-	-	4''	1.17	-2.06

Bis-formamide **9**

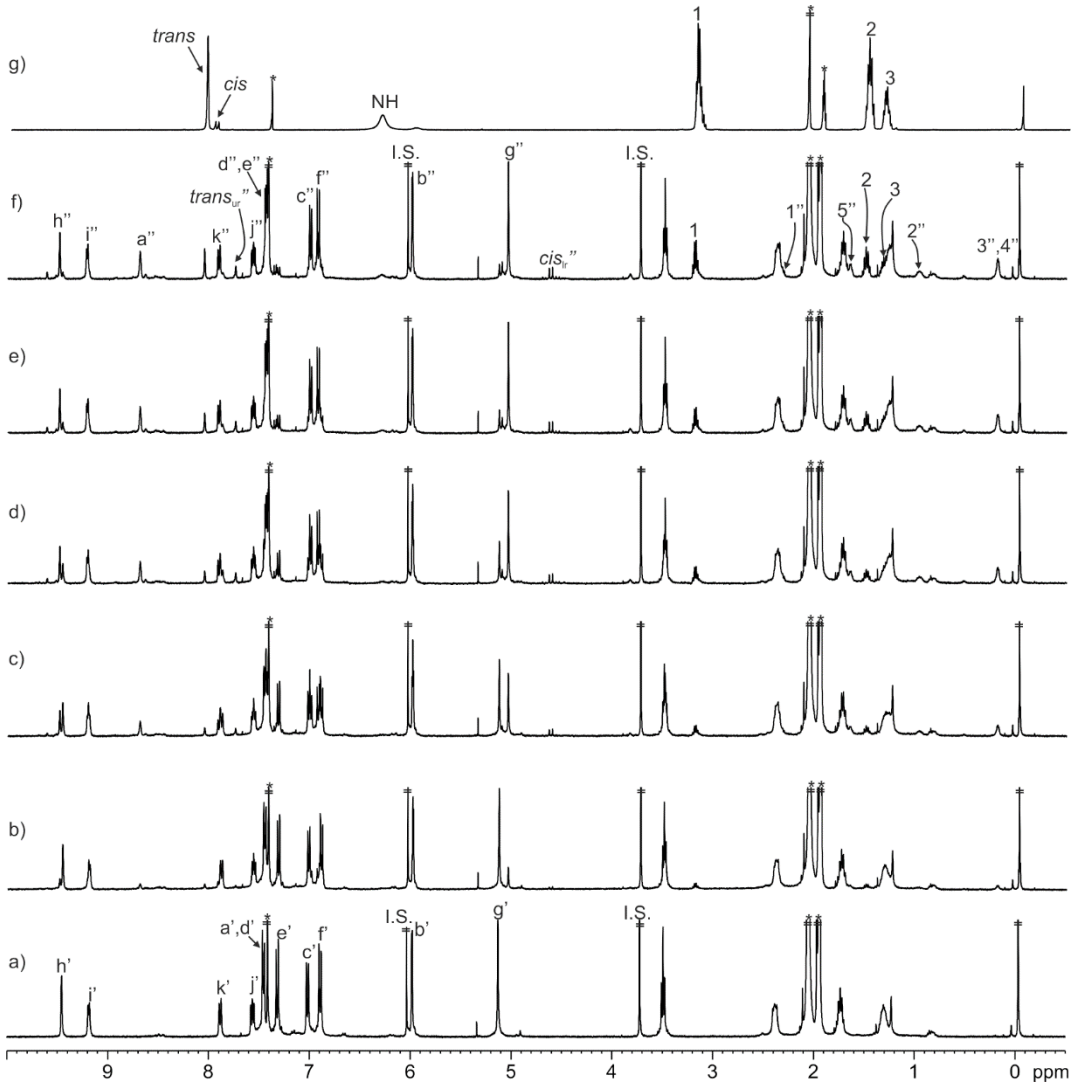

Figure S23. ^{1}H NMR (400 MHz, 2:1 $CDCl_3/CD_3CN$, 298 K) spectra of the titration of [**1b**•Pd]$^{2+}$ with **9**: a) 0; b) 0.5; c) 1; d) 1.5; e) 2 and f) 2.5 equiv.; g) **9**. Primed labels correspond to proton signals of [**1b**•Pd]$^{2+}$. Doubly primed labels correspond to proton signals of *trans,cis*-**9**⊂[**1b**•Pd]$^{2+}$. See Scheme S1 and Figure S29 for proton assignments. 1,3,5-Trimethoxybenzene (I.S.). *Residual solvent peaks.

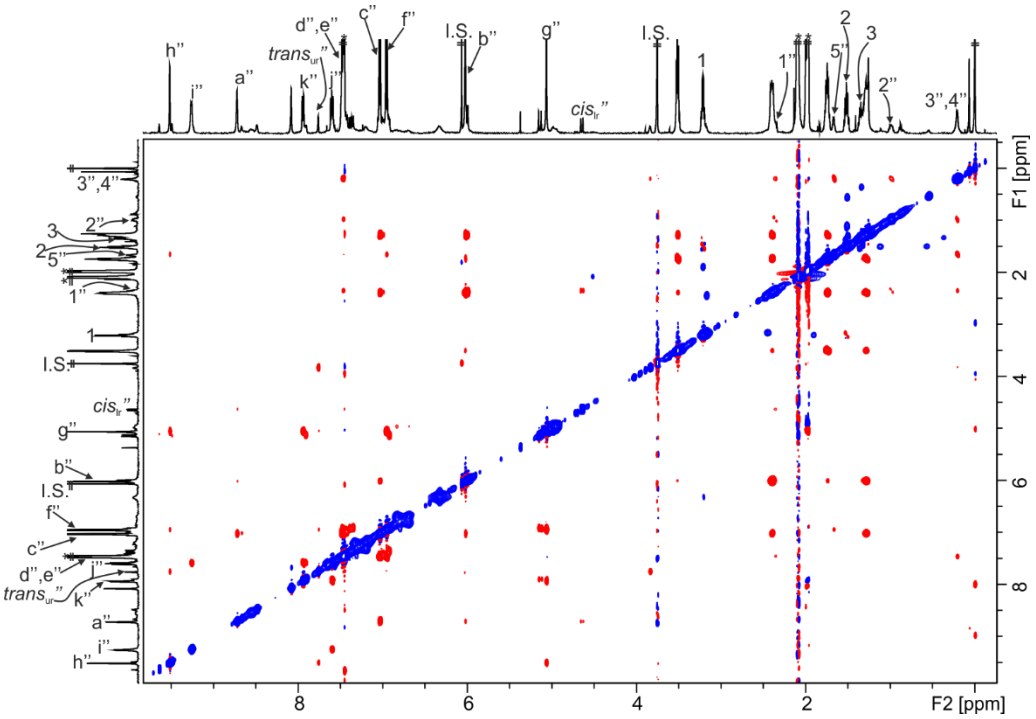

Figure S24. ^{1}H-^{1}H ROESY NMR (500 MHz with cryoprobe, 2:1 $CDCl_3/CD_3CN$, 298 K, spin lock = 0.3 s) spectrum of [**1b**•Pd]$^{2+}$ with 2.5 equiv. of **9**. See Figure S29 for proton assignment. *Residual solvent peaks.

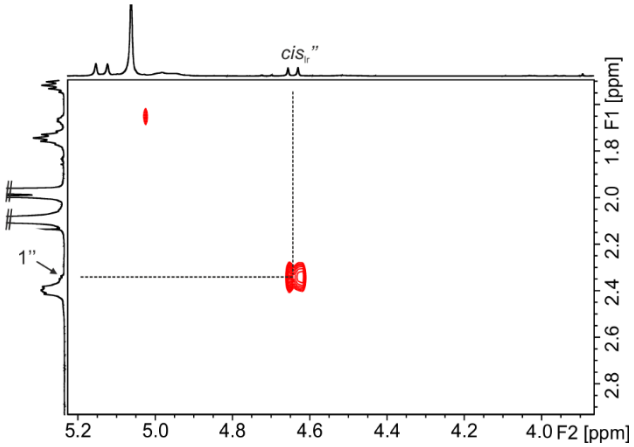

Figure S25. Selected region of the ^{1}H-^{1}H ROESY NMR (500 MHz with cryoprobe, 2:1 $CDCl_3/CD_3CN$, 298 K, spin lock = 0.3 s) spectrum of [**1b**•Pd]$^{2+}$ with 2.5 equiv. of **9**. The ROESY cross-peak between 1'' and the signal at 4.61 ppm is highlighted. The observed cross-peak confirms that one of the formamide groups of bound **9** adopts a *cis*-conformation. See Figure S29 for proton assignment.

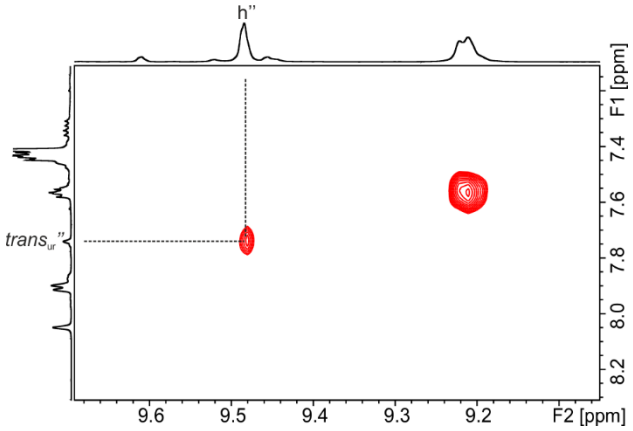

Figure S26. Selected region of the ^{1}H-^{1}H ROESY NMR (500 MHz with cryoprobe, 2:1 $CDCl_3/CD_3CN$, 298 K, spin lock = 0.3 s) spectrum of [**1b**•Pd]$^{2+}$ with 2.5 equiv. of **9**. The ROESY cross-peak between h'' and *trans*$_{ur}$'' is highlighted. The observed cross-peak indicates that one of the formamide groups of bound *trans,cis*-**9** is located in the binding site defined by the inwardly-directed *α*-pyridyl protons. See Scheme S1 and Figure S29 for proton assignments.

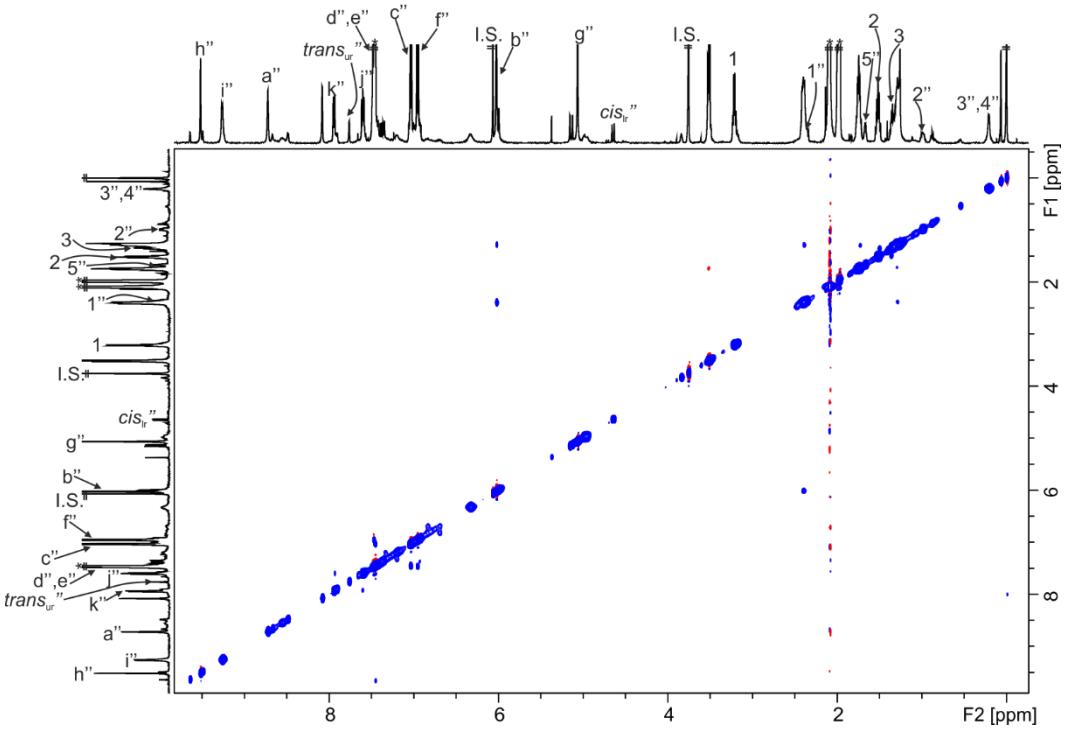

Figure S27. ^{1}H-^{1}H EXSY NMR (500 MHz with cryoprobe, 2:1 $CDCl_3/CD_3CN$, 298 K, mixing time = 0.3 s) spectrum of [**1b**•Pd]$^{2+}$ with 2.5 equiv. of **9**. See Figure S15 and Figure S29 for proton assignments. *Residual solvent peaks.

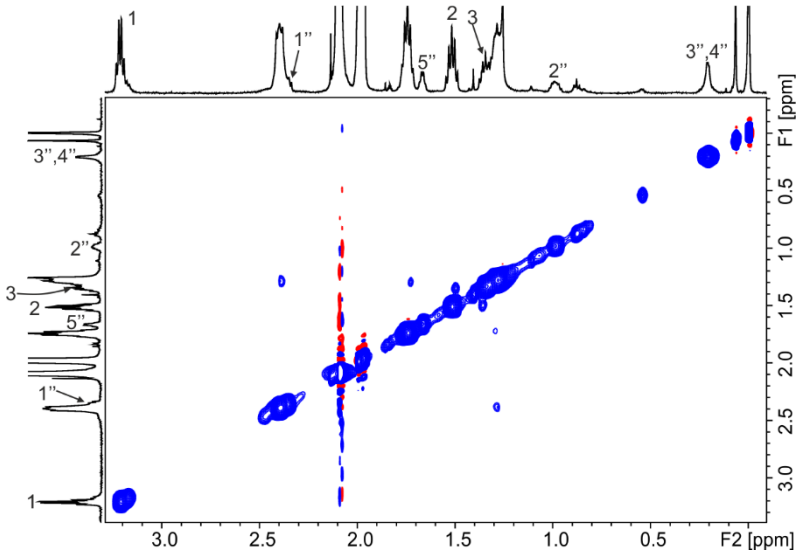

Figure S28. Selected region of the ^{1}H-^{1}H EXSY NMR (500 MHz with cryoprobe, 2:1 $CDCl_3/CD_3CN$, 298 K, mixing time = 0.3 s) spectrum of [**1b**•Pd]$^{2+}$ with 2.5 equiv. of **9**. See Figure S15 and Figure S29 for proton assignments.

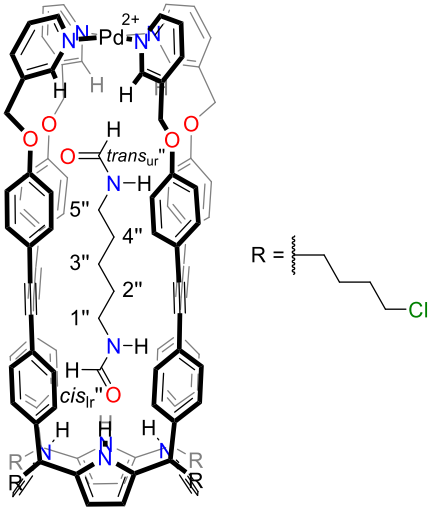

Figure S29. Line-drawing structure of the *trans*,*cis*-**9**⊂[**1b**•Pd]$^{2+}$ cage complex.

Table S2. Experimental chemical shifts of free (δ_{free}) and bound (δ_{bound}) *bis*-formamide **9** and complexation-induced shifts ($\Delta\delta$).

Signal	δ_{free} (ppm)	Signal	δ_{bound} (ppm)	$\Delta\delta$ (ppm)
trans	8.08	*trans*$_{ur}$''	7.76	-0.32
cis	7.99	*cis*$_{lr}$''	4.61	-3.38
1	3.21	1''	2.36	-0.85
2	1.52	2''	0.99	-0.53
3	1.34	3''	0.21	-1.13
-	-	4''	0.21	-1.31
-	-	5''	1.67	-1.54

Mono-formamide **10**

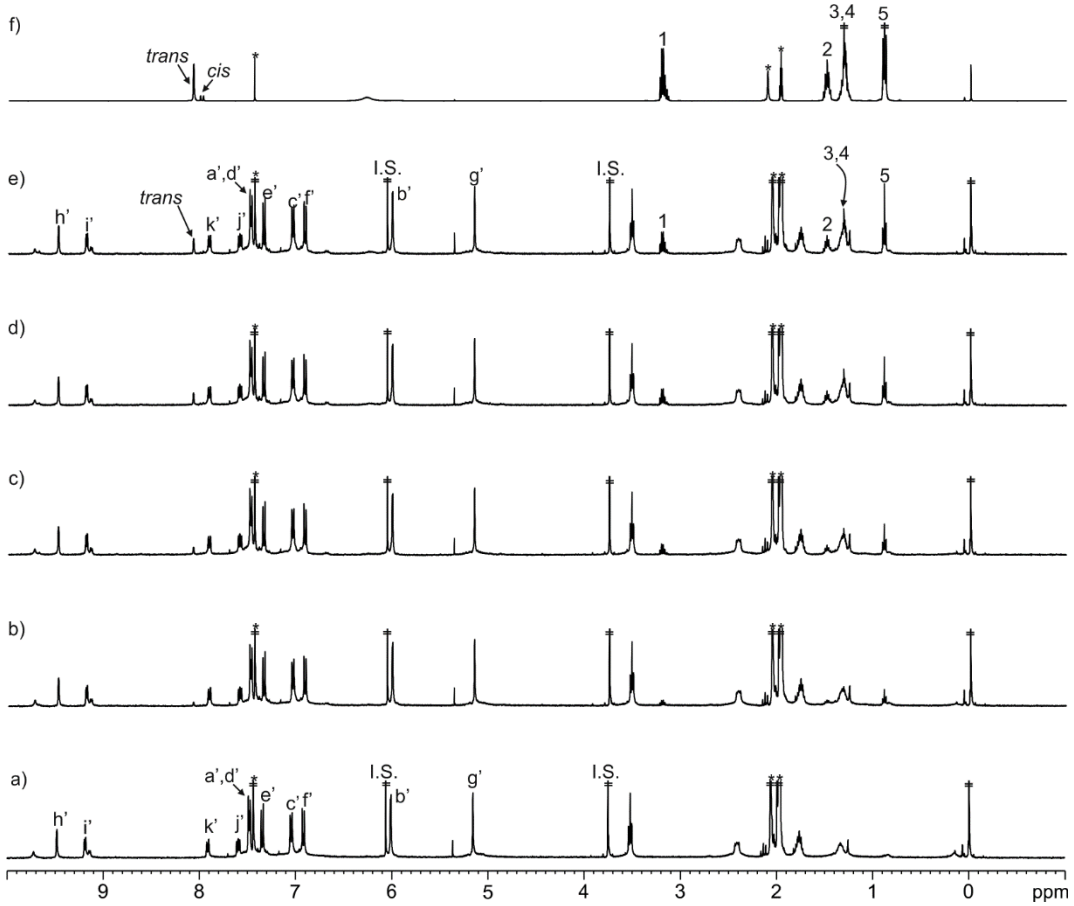

Figure S30. ^{1}H NMR (400 MHz, 2:1 $CDCl_3/CD_3CN$, 298 K) spectra of the titration of [**1b**•Pd]$^{2+}$ with **10**: a) 0; b) 0.5; c) 1; d) 1.5 and e) 2 equiv.; f) **10**. Primed labels correspond to proton signals of [**1b**•Pd]$^{2+}$. See Scheme S1 and Figure S15 for proton assignments. 1,3,5-Trimethoxybenzene (I.S.). *Residual solvent peaks.

The addition of 2 equiv. of *mono*-formamide **10** to a millimolar solution of [**1b**•Pd]$^{2+}$ in 2:1 $CDCl_3/CD_3CN$ did not produce noticeable changes in the proton signals of the Pd(II)-cage.

5. Self-assembly of [2•Pd]$^{6+}$ using *N*-oxides and formamides (5-10), 2D NMR spectra of cage complexes and DOSY experiments

A suspension of the tetra-cationic tetra-pyridyl SAE-C[4]P **2**$^{4+}$ (1 mM) and *tert*-butanol (internal standard, 1 mM) was prepared in D_2O solution. The suspension was heated at 50-60°C for 1 h leading to a clear solution. A solution of the guest (**5**-**10**) was prepared in D_2O solution at higher concentration (10-20 mM). Immediately, the guest (1-2 equiv.) was added to the tetra-cationic tetra-pyridyl's solution. After that, 0.5 mL of the solution were placed in an NMR tube and variable-temperature (VT) ^{1}H NMR experiments were performed (see figure footnotes for details). A solution of $Pd(NO_3)_2$ salt was prepared in D_2O solution at higher concentration (10-30 mM). Subsequently, Pd(II) (*ca.* 1 equiv.) was added to the D_2O solution containing the tetra-cationic tetra-pyridyl **2**$^{4+}$ and the guest. VT ^{1}H NMR experiments (see figure footnotes for details) were performed after vigorous hand shaking of the NMR tube for few seconds.

5.1 Attempts to self-assemble the [2•Pd]$^{6+}$ cage in the absence of guests

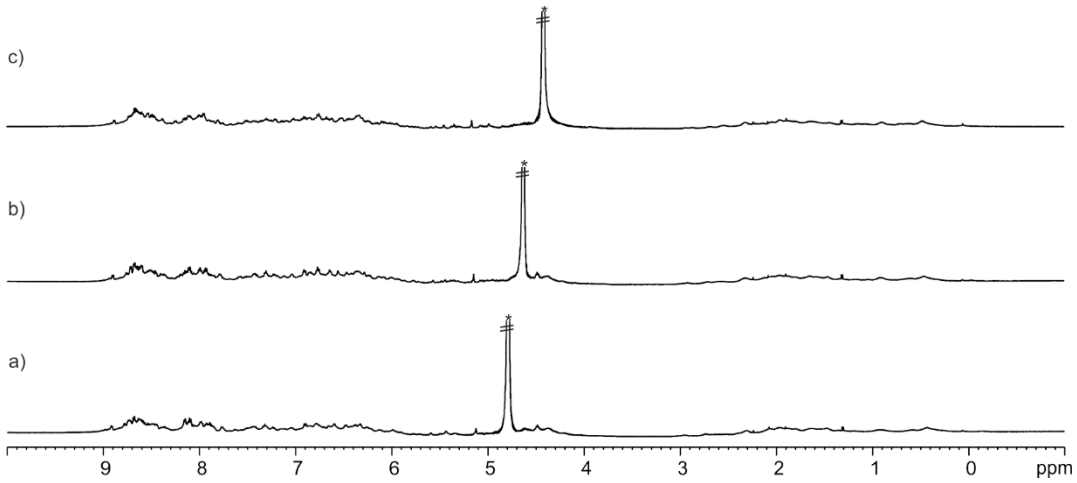

Figure S31. VT ^{1}H NMR (500 MHz with cryoprobe, D_2O) spectra of **2**$^{4+}$: a) 298; b) 313 and c) 333 K. *Residual solvent peak.

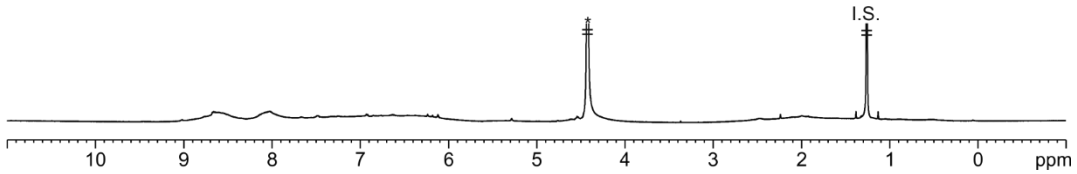

Figure S32. ^{1}H NMR (500 MHz with cryoprobe, D_2O, 333 K) spectrum of **2**$^{4+}$ with *ca.* 1 equiv. of $Pd(NO_3)_2$. *tert*-Butanol (I.S.). *Residual solvent peak.

5.2 Self-assembly of the [2•Pd]$^{6+}$ cage in the presence of pyridine *N*-oxides 5, 6 and 7

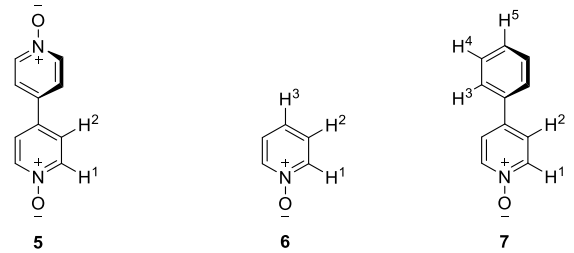

5 **6** **7**

Figure S33. Line-drawing structures of pyridine *N*-oxides **5**, **6** and **7**.

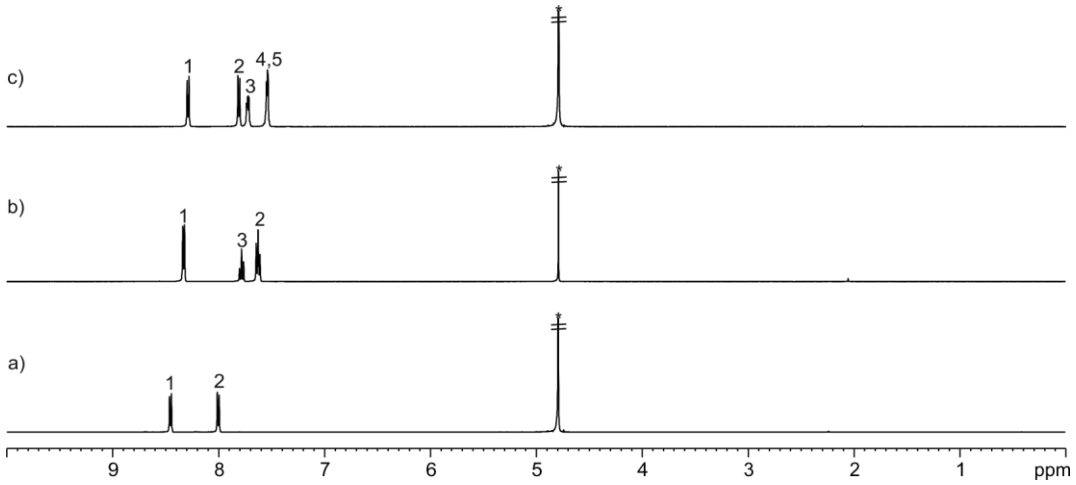

Figure S34. ^{1}H NMR (400 MHz, D_2O, 298 K) spectra of: a) **5**; b) **6** and c) **7**. See Figure S33 for proton assignments. *Residual solvent peak.

Bis-N-oxide **5**

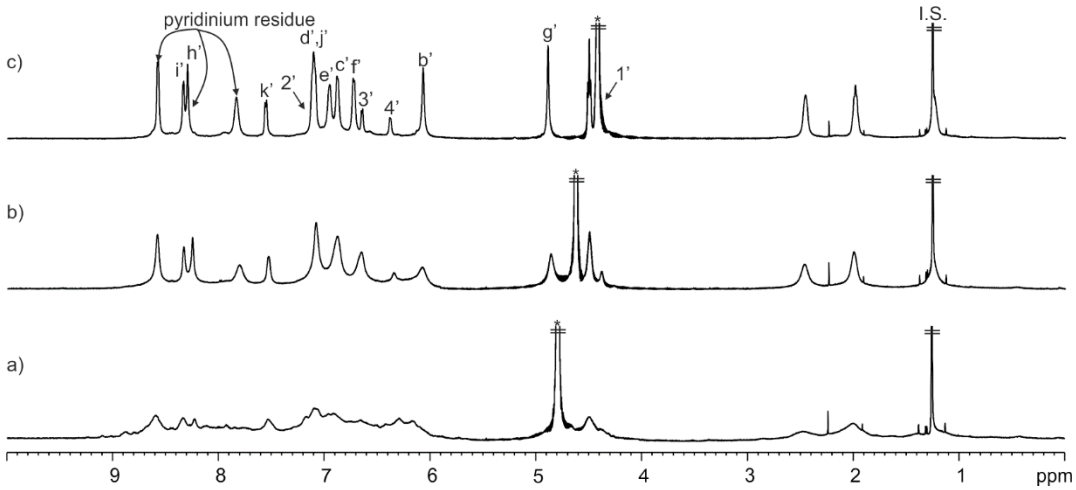

Figure S35. VT ^{1}H NMR (500 MHz with cryoprobe, D_2O) spectra of $\mathbf{2}^{4+}$ with *ca.* 1 equiv. of **5**: a) 298; b) 313 and c) 333 K. Primed labels correspond to proton signals of $\mathbf{5}\subset\mathbf{2}^{4+}$. See Scheme S2 and Figure S33 for proton assignments. *tert*-Butanol (I.S.). *Residual solvent peak.

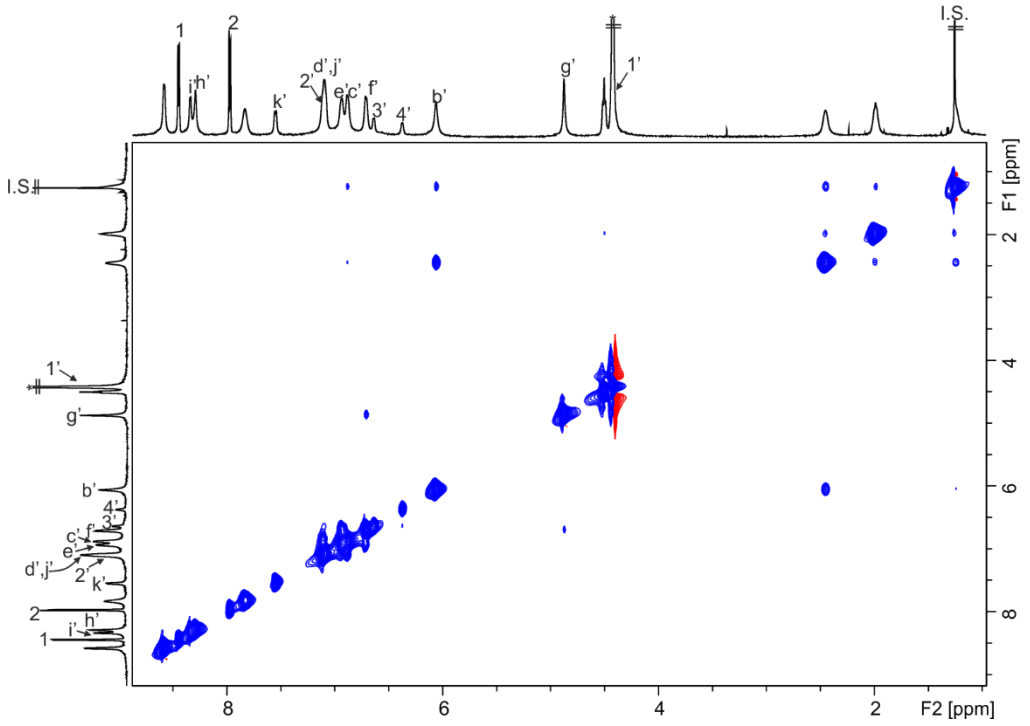

Figure S36. ^{1}H-^{1}H EXSY NMR (500 MHz with cryoprobe, D_2O, 333 K, mixing time = 0.3 s) spectrum of $\mathbf{2}^{4+}$ with ca. 2 equiv. of **5**. See Scheme S2 and Figure S33 for proton assignments. *Residual solvent peak.

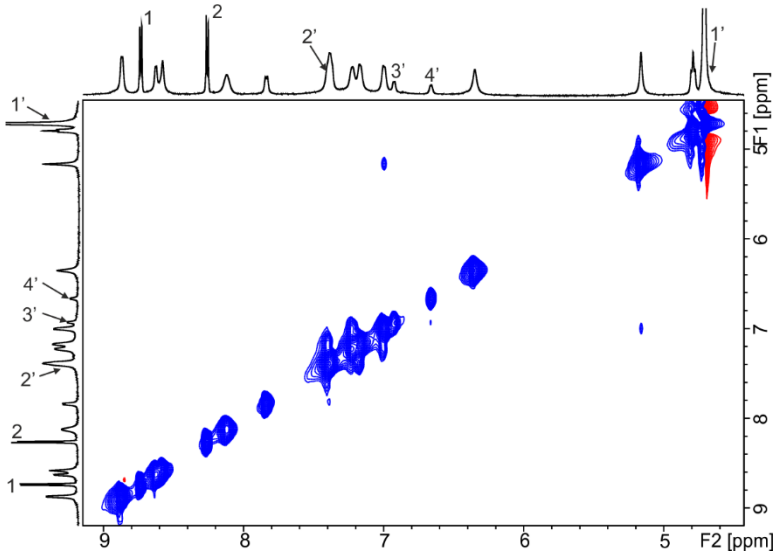

Figure S37. Selected region of the ^{1}H-^{1}H EXSY NMR (500 MHz with cryoprobe, D_2O, 333 K, mixing time = 0.3 s) spectrum of $\mathbf{2}^{4+}$ with *ca.* 2 equiv. of **5**. See Scheme S2 and Figure S33 for proton assignments.

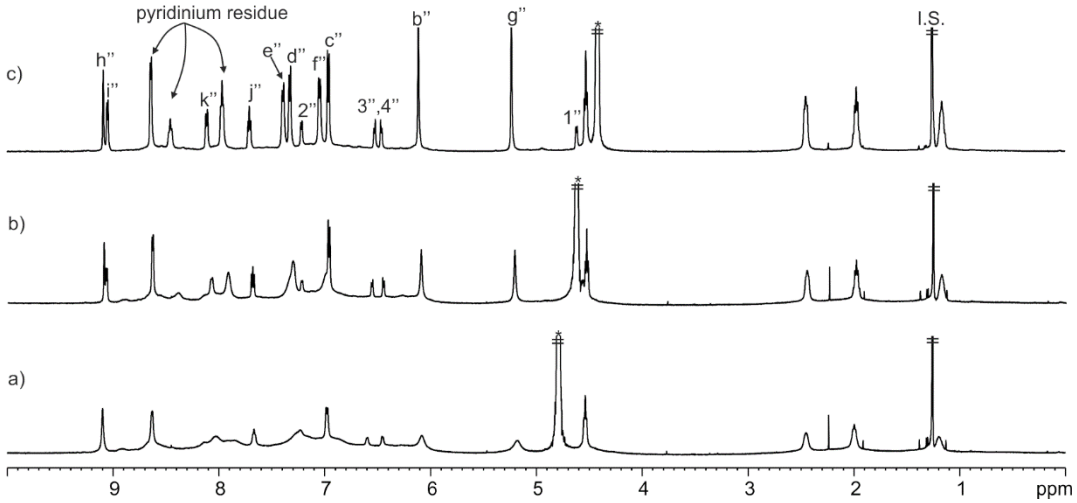

Figure S38. VT ^{1}H NMR (500 MHz with cryoprobe, D_2O) spectra of $\mathbf{2}^{4+}$ with *ca.* 1 equiv. of **5** upon the addition of *ca.* 1 equiv. of Pd(II): a) 298; b) 313 and c) 333 K. Doubly primed labels correspond to proton signals of $\mathbf{5}\subset[\mathbf{2}\bullet Pd]^{6+}$. The $\mathbf{5}\subset[\mathbf{2}\bullet Pd]^{6+}$ cage complex was assembled in 60% extent. See Scheme S2 and Figure S42 for proton assignments. *tert*-Butanol (I.S.). *Residual solvent peak.

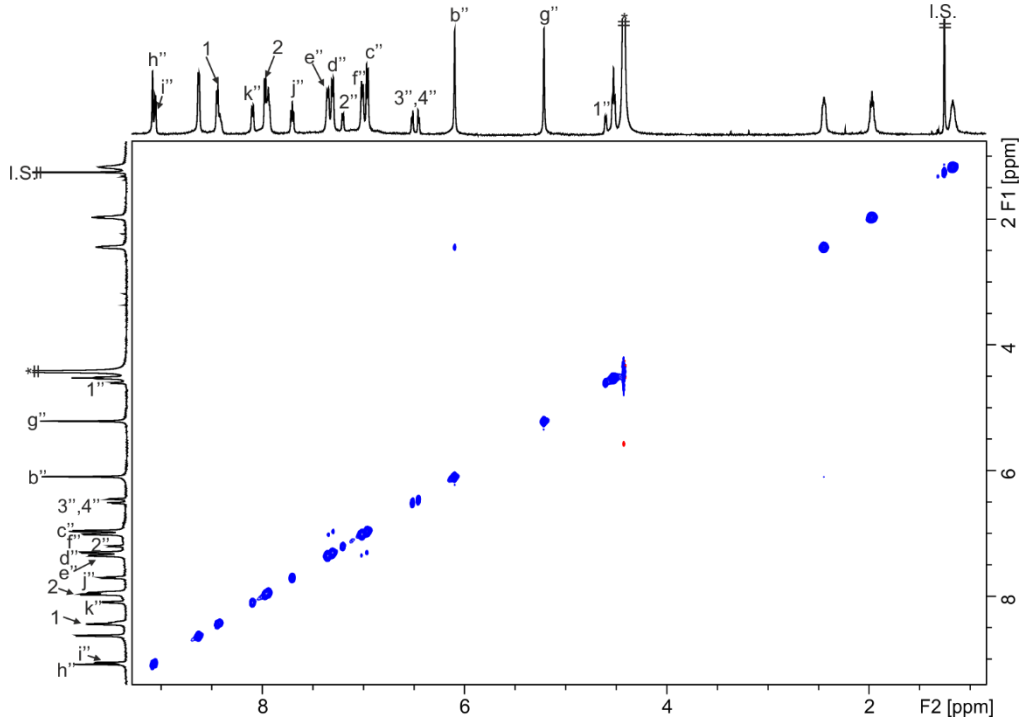

Figure S39. ^{1}H-^{1}H EXSY NMR (500 MHz with cryoprobe, D_2O, 333 K, mixing time = 0.3 s) spectrum of $[\mathbf{2}\bullet Pd]^{6+}$ with *ca.* 2 equiv. of **5**. See Figure S33 and Figure S42 for proton assignments. *Residual solvent peak.

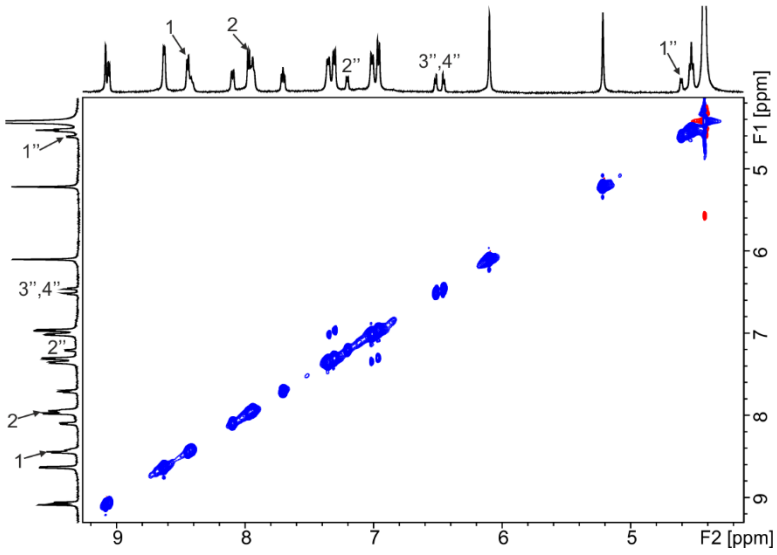

Figure S40. Selected region of the ^{1}H-^{1}H EXSY NMR (500 MHz with cryoprobe, D_2O, 333 K, mixing time = 0.3 s) spectrum of [**2**•Pd]$^{6+}$ with *ca.* 2 equiv. of **5**. See Figure S33 and Figure S42 for proton assignments.

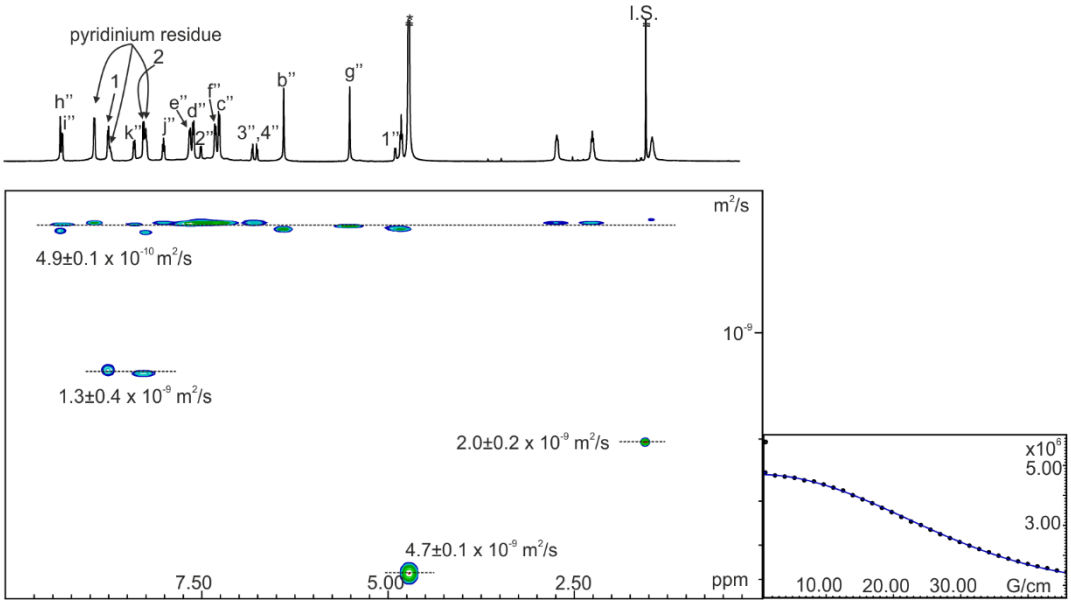

Figure S41. left) ^{1}H pseudo 2D DOSY (500 MHz with cryoprobe, D_2O, 333 K, D20 = 0.20 s; P30 = 0.60 ms) of [**2**•Pd]$^{6+}$ with *ca.* 2 equiv. of **5**. right) Fit of the decay of the signal b'' to a mono-exponential function using Dynamics Center from Bruker. Doubly primed labels correspond to proton signals of **5**⊂[**2**•Pd]$^{6+}$. See Scheme S2, Figure S33 and Figure S42 for proton assignments. Errors are indicated as standard deviations. *tert*-Butanol (I.S.). *Residual solvent peak.

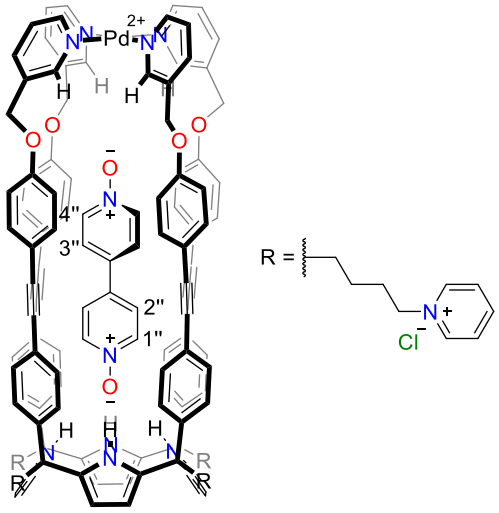

Figure S42. Line-drawing structure of the **5**⊂[**2**•Pd]$^{6+}$ cage complex.

Table S3. Experimental chemical shifts of free (δ_{free}) and bound (δ_{bound}) *bis-N*-oxide **5** and complexation-induced shifts ($\Delta\delta$).

Signal	δ_{free} (ppm)	Signal	δ_{bound} (ppm)	$\Delta\delta$ (ppm)
1	8.45	1''	4.62	-3.83
2	7.97	2''	7.22	-0.75
-	-	3''	6.48	-1.49
-	-	4''	6.48	-1.97

Pyridine *N*-oxide **6**

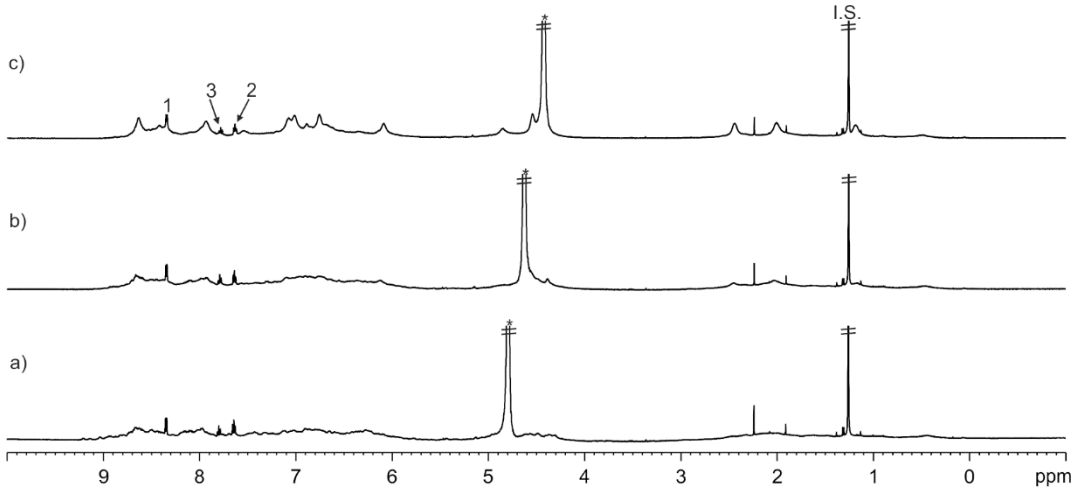

Figure S43. VT ^{1}H NMR (500 MHz with cryoprobe, D_2O) spectra of **2**$^{4+}$ with *ca.* 1 equiv. of **6**: a) 298; b) 313 and c) 333 K. See Figure S33 for proton assignment. *tert*-Butanol (I.S.). *Residual solvent peak.

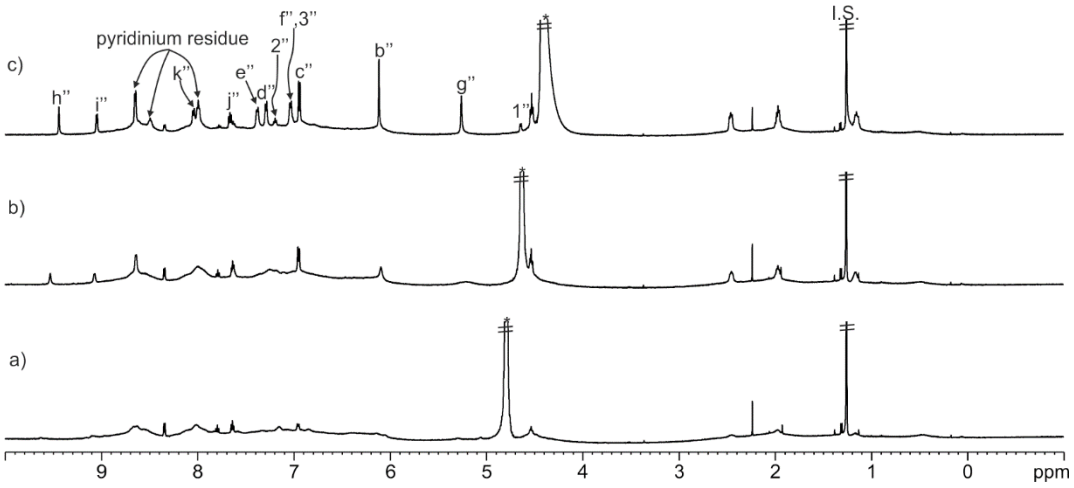

Figure S44. VT ^{1}H NMR (500 MHz with cryoprobe, D_2O) spectra of $\mathbf{2}^{4+}$ with *ca.* 1 equiv. of **6** upon the addition of *ca.* 1 equiv. of Pd(II): a) 298; b) 313 and c) 333 K. Doubly primed labels correspond to proton signals of $\mathbf{6}\subset[\mathbf{2}\bullet Pd]^{6+}$. The $\mathbf{6}\subset[\mathbf{2}\bullet Pd]^{6+}$ cage complex was assembled in 30% extent. See Scheme S2 and Figure S46 for proton assignments. *tert*-Butanol (I.S.). *Residual solvent peak.

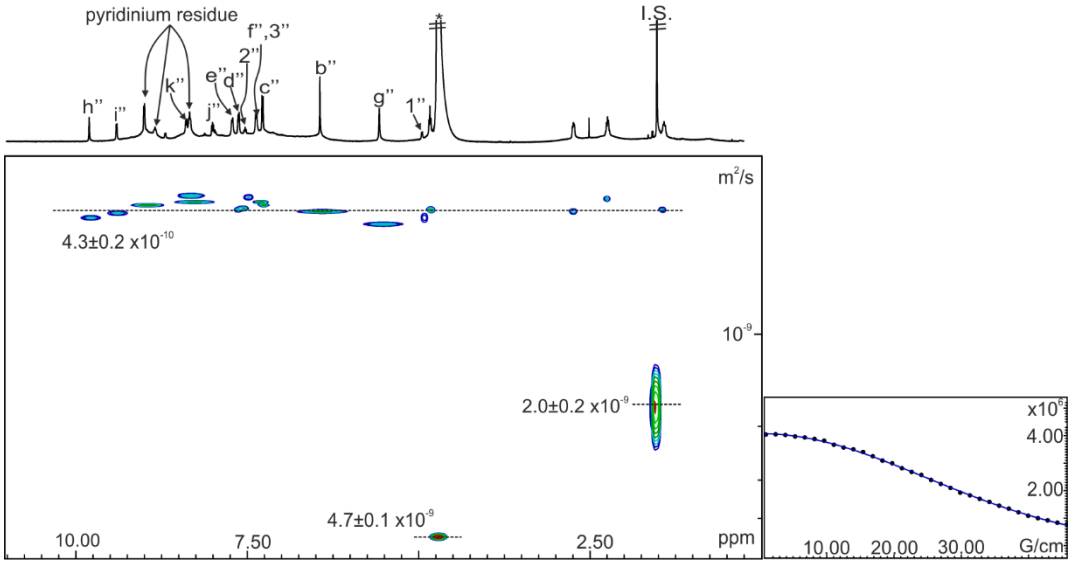

Figure S45. left) ^{1}H pseudo 2D DOSY (500 MHz with cryoprobe, D_2O, 333 K, D20 = 0.20 s; P30 = 0.60 ms) of $[\mathbf{2}\bullet Pd]^{6+}$ with *ca.* 1 equiv. of **6**. right) Fit of the decay of the signal b'' to a mono-exponential function using Dynamics Center from Bruker. Doubly primed labels correspond to proton signals of $\mathbf{6}\subset[\mathbf{2}\bullet Pd]^{6+}$. See Scheme S2, Figure S33 and Figure S46 for proton assignments. Errors are indicated as standard deviations. *tert*-Butanol (I.S.). *Residual solvent peak.

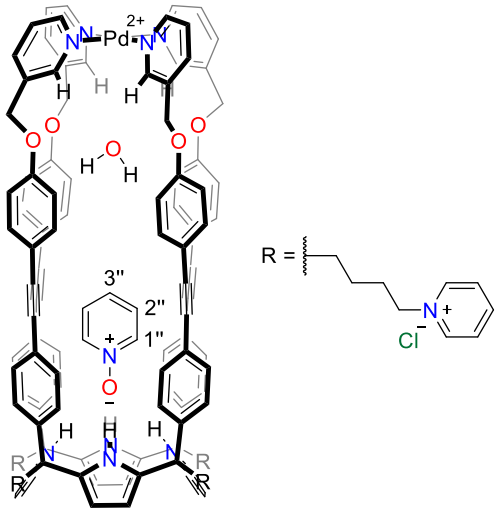

Figure S46. Line-drawing structure of the putative [**6**•H_2O]⊂[**2**•Pd]$^{6+}$ cage complex.

Table S4. Experimental chemical shifts of free (δ_{free}) and bound (δ_{bound}) pyridine *N*-oxide **6** and complexation-induced shifts ($\Delta\delta$).

Signal	δ_{free} (ppm)	Signal	δ_{bound} (ppm)	$\Delta\delta$ (ppm)
1	8.34	1''	4.61	-3.73
2	7.61	2''	7.17	-0.44
3	7.77	3''	7.04	-0.73

4-Phenylpyridine *N*-oxide **7**

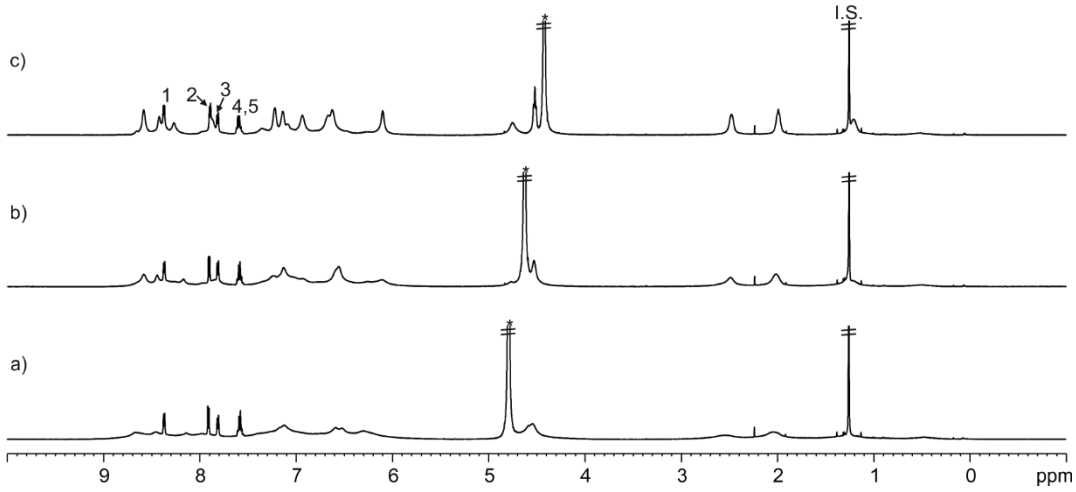

Figure S47. VT ^{1}H NMR (500 MHz with cryoprobe, D_2O) spectra of **2**$^{4+}$ with *ca.* 1 equiv. of **7**: a) 298; b) 313 and c) 333 K. See Figure S33 for proton assignment. *tert*-Butanol (I.S.). *Residual solvent peak.

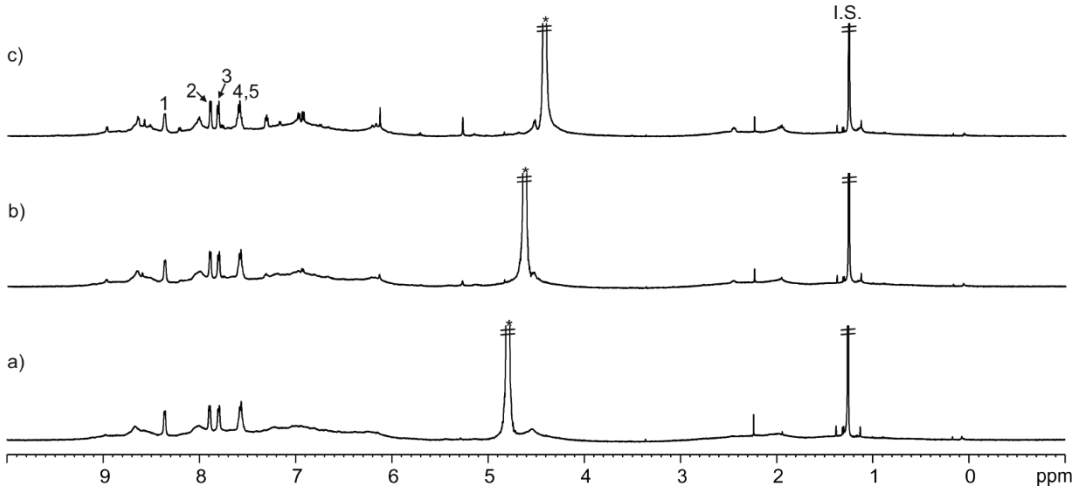

Figure S48. VT ^{1}H NMR (500 MHz with cryoprobe, D_2O) spectra of $\mathbf{2}^{4+}$ with *ca.* 1 equiv. of **7** upon the addition of *ca.* 1 equiv. of Pd(II): a) 298; b) 313 and c) 333 K. See Figure S33 for proton assignment. *tert*-Butanol (I.S.). *Residual solvent peak.

The addition of *ca.* 1 equiv. of Pd(II) to the equimolar solution of **7** and $\mathbf{2}^{4+}$ provoked the formation of polymeric aggregates to a significant extent.

5.3 Self-assembly of the [2•Pd]$^{6+}$ cage in the presence of formamides 8, 9 and 10

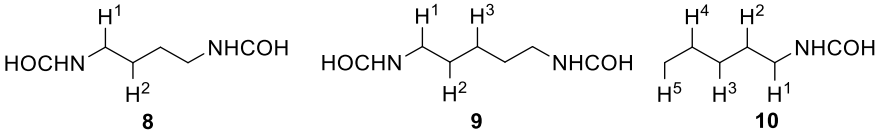

Figure S49. Line-drawing structures of formamides **8**, **9** and **10**.

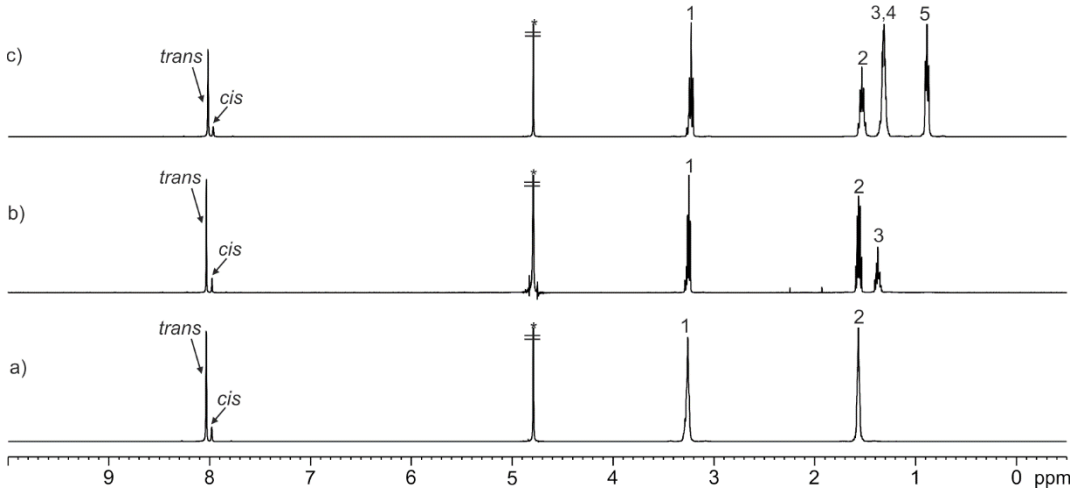

Figure S50. ^{1}H NMR (400 MHz, D_2O, 298 K) spectra of: a) **8**; b) **9** and c) **10**. See Figure S49 for proton assignments. *Residual solvent peak.

Bis-formamide **8**

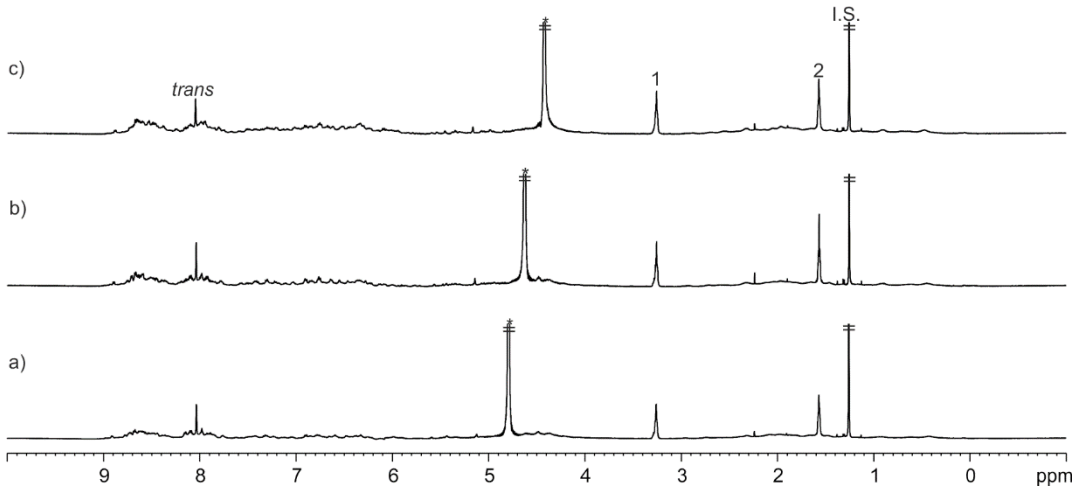

Figure S51. VT ^{1}H NMR (500 MHz with cryoprobe, D_2O) spectra of $\mathbf{2}^{4+}$ with *ca.* 1 equiv. of **8**: a) 298; b) 313 and c) 333 K. See Figure S49 for proton assignment. *tert*-Butanol (I.S.). *Residual solvent peak.

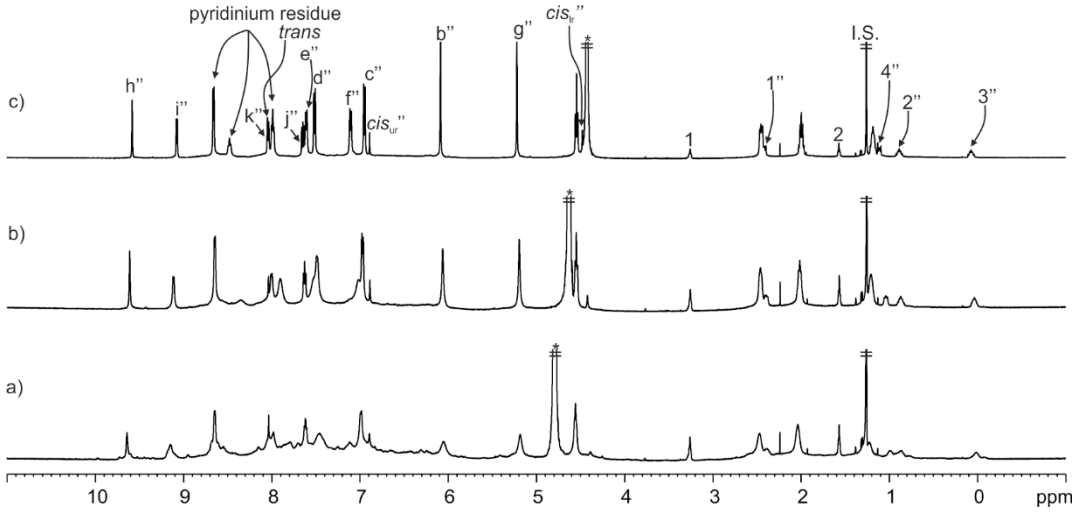

Figure S52. VT ^{1}H NMR (500 MHz with cryoprobe, D_2O) spectra of $\mathbf{2}^{4+}$ with *ca.* 1 equiv. of **8** upon the addition of *ca.* 1 equiv. of Pd(II): a) 298; b) 313 and c) 333 K. Doubly primed labels correspond to proton signals of *cis*,*cis*-**8**⊂[**2**•Pd]$^{6+}$. The *cis,cis*-**8**⊂[**2**•Pd]$^{6+}$ cage complex was assembled in 60% extent. See Scheme S2 and Figure S59 for proton assignments. *tert*-Butanol (I.S.). *Residual solvent peak.

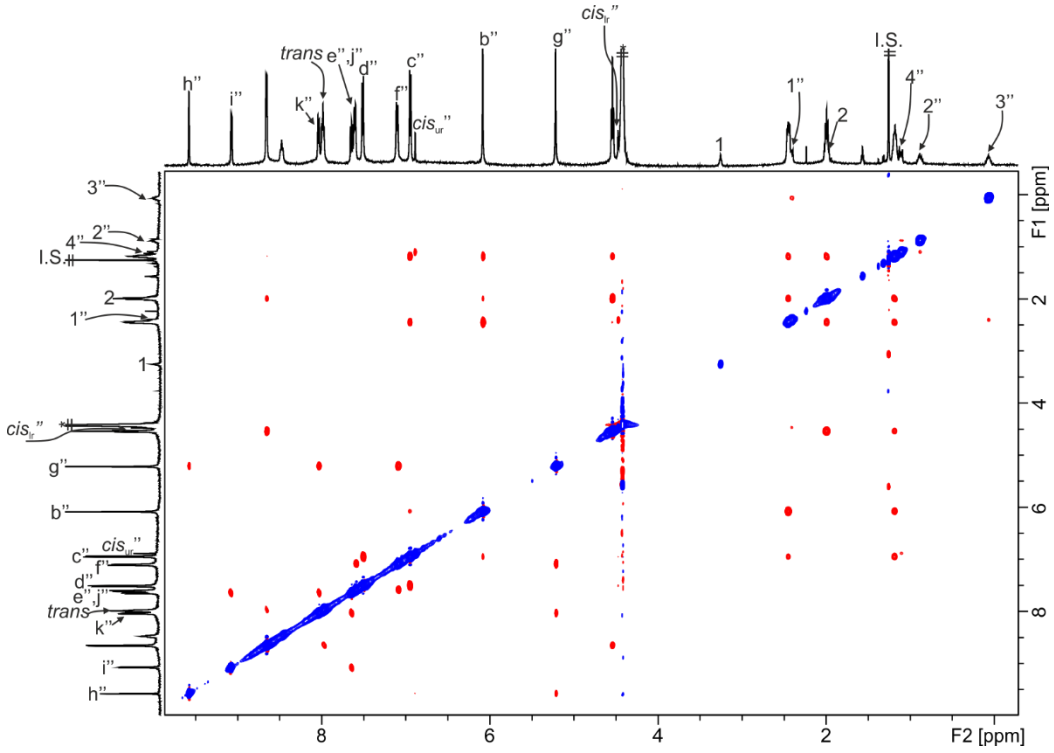

Figure S53. ^{1}H-^{1}H ROESY NMR (500 MHz with cryoprobe, D_2O, 333 K, spin lock = 0.3 s) spectrum of [**2**•Pd]$^{6+}$ with *ca.* 1 equiv. of **8**. See Figure S59 for proton assignment. *Residual solvent peak.

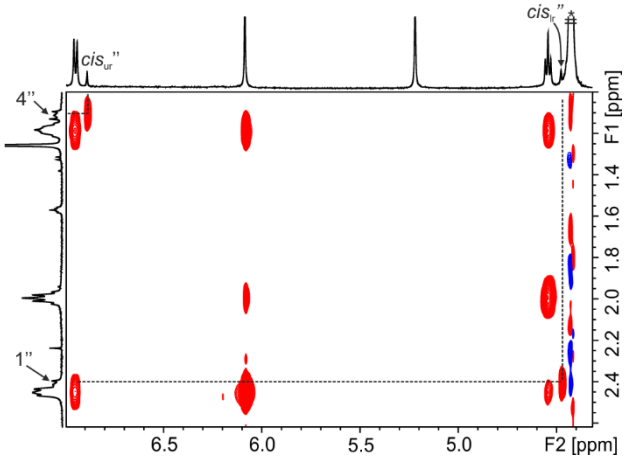

Figure S54. Selected region of the ^{1}H-^{1}H ROESY NMR (500 MHz with cryoprobe, D_2O, 333 K, spin lock = 0.3 s) spectrum of [**2**•Pd]$^{6+}$ with *ca.* 1 equiv. of **8**. The ROESY cross-peaks between 1'' and 4'' with the signals at 4.48 and 6.89 ppm, respectively, are highlighted. The observed cross-peaks confirm that the two formamide groups of bound **8** adopt a *cis*-conformation. See Figure S59 for proton assignment.

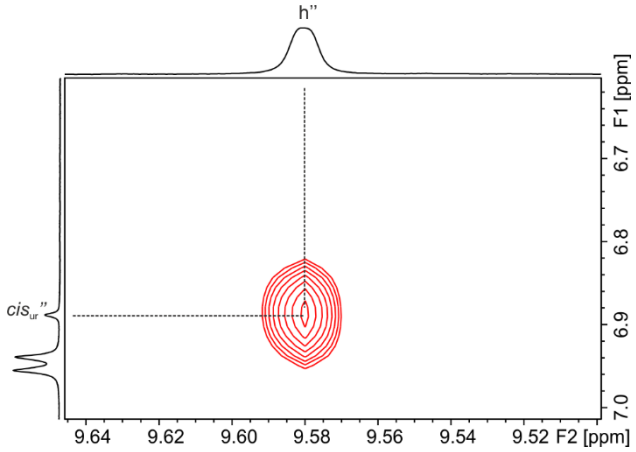

Figure S55. Selected region of the ^{1}H-^{1}H ROESY NMR (500 MHz with cryoprobe, D_2O, 333 K, spin lock = 0.3 s) spectrum of [**2**•Pd]$^{6+}$ with *ca.* 1 equiv. of **8**. The ROESY cross-peak between h'' and *cis*$_{ur}$'' is highlighted. The observed cross-peak indicates that one of the formamide groups of bound *cis*,*cis*-**8** is located in the binding site defined by the inwardly-directed *α*-pyridyl protons. See Scheme S2 and Figure S59 for proton assignments.

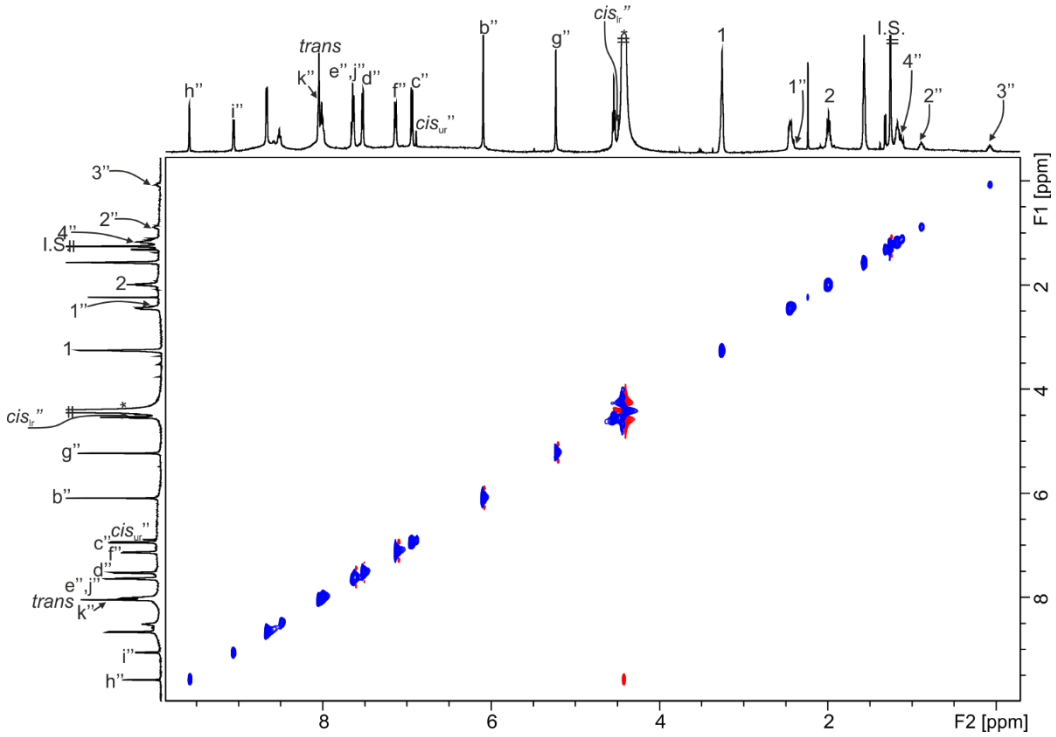

Figure S56. ^{1}H-^{1}H EXSY NMR (500 MHz with cryoprobe, D_2O, 333 K, mixing time = 0.3 s) spectrum of [**2**•Pd]$^{6+}$ with *ca.* 2 equiv. of **8**. See Figure S49 and Figure S59 for proton assignments. *Residual solvent peak.

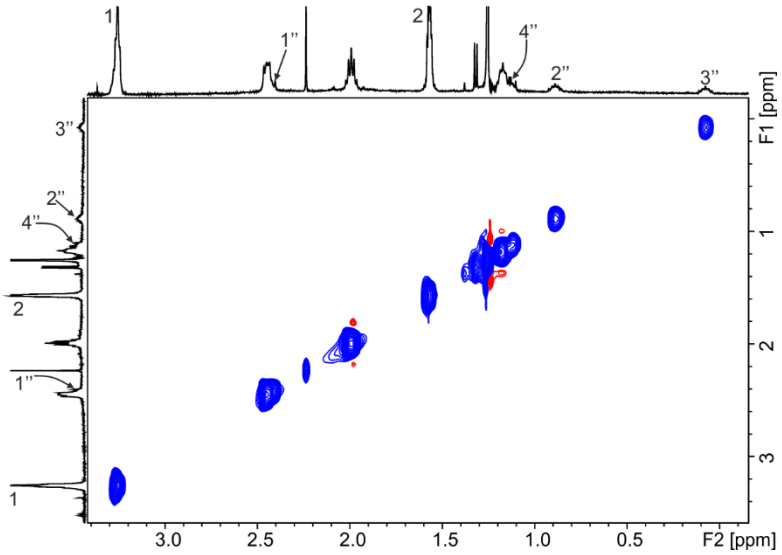

Figure S57. Selected region of the ^{1}H-^{1}H EXSY NMR (500 MHz with cryoprobe, D_2O, 333 K, mixing time = 0.3 s) spectrum of [**2**•Pd]$^{6+}$ with *ca.* 2 equiv. of **8**. See Figure S49 and Figure S59 for proton assignments.

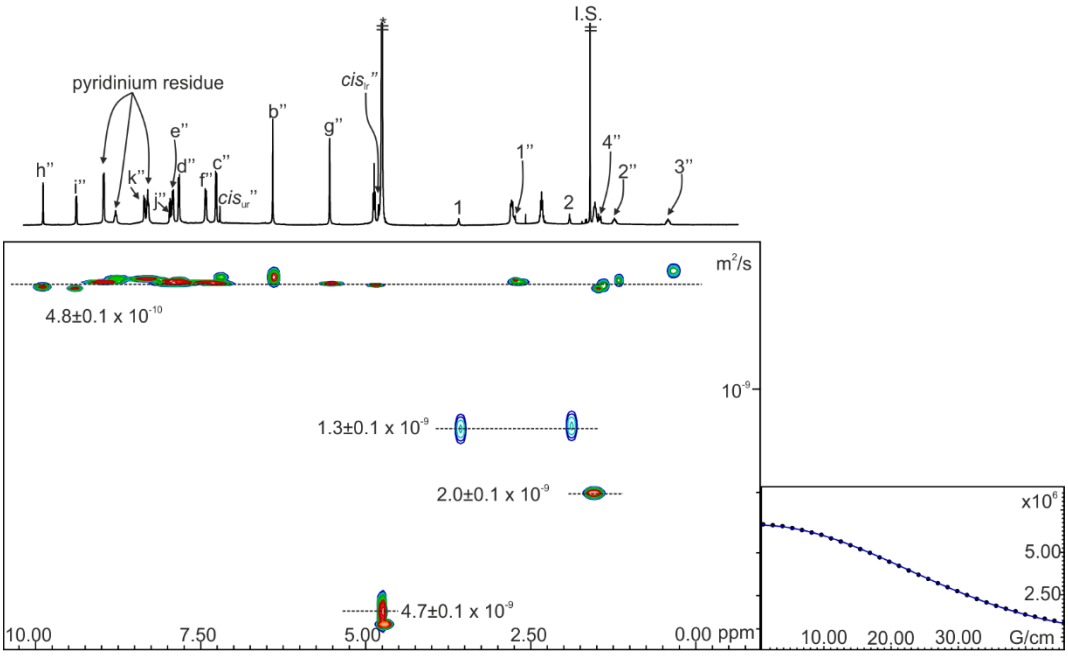

Figure S58. left) ^{1}H pseudo 2D DOSY (500 MHz with cryoprobe, D_2O, 333 K, D20 = 0.20 s; P30 = 0.60 ms) of [**2**•Pd]$^{6+}$ with *ca.* 1 equiv. of **8**. right) Fit of the decay of the signal b'' to a mono-exponential function using Dynamics Center from Bruker. Doubly primed labels correspond to proton signals of *cis*,*cis*-**8**⊂[**2**•Pd]$^{6+}$. See Scheme S2, Figure S49 and Figure S59 for proton assignments. Errors are indicated as standard deviations. *tert*-Butanol (I.S.). *Residual solvent peak.

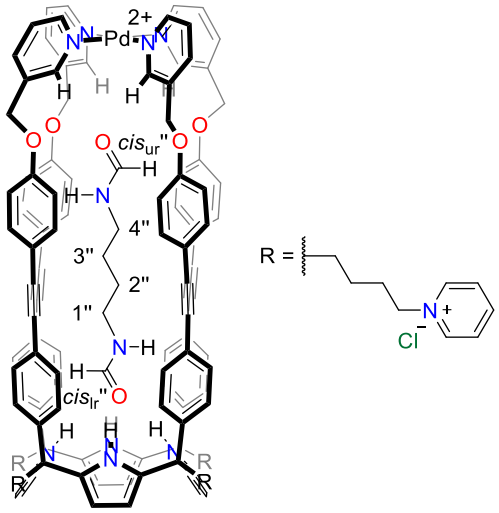

Figure S59. Line-drawing structure of the *cis*,*cis*-**8**⊂[**2**•Pd]$^{6+}$ cage complex.

Table S5. Experimental chemical shifts of free (δ_{free}) and bound (δ_{bound}) *bis*-formamide **8** and complexation-induced shifts ($\Delta\delta$).

Signal	δ_{free} (ppm)	Signal	δ_{bound} (ppm)	$\Delta\delta$ (ppm)
trans	8.05	-	-	-
cis	8.00	*cis*$_{lr}$''	4.48	-3.52
-	-	*cis*$_{ur}$''	6.89	-1.11
1	3.26	1''	2.41	-0.85
2	1.57	2''	0.89	-0.68
-	-	3''	0.07	-1.50
-	-	4''	1.11	-2.15

Bis-formamide **9**

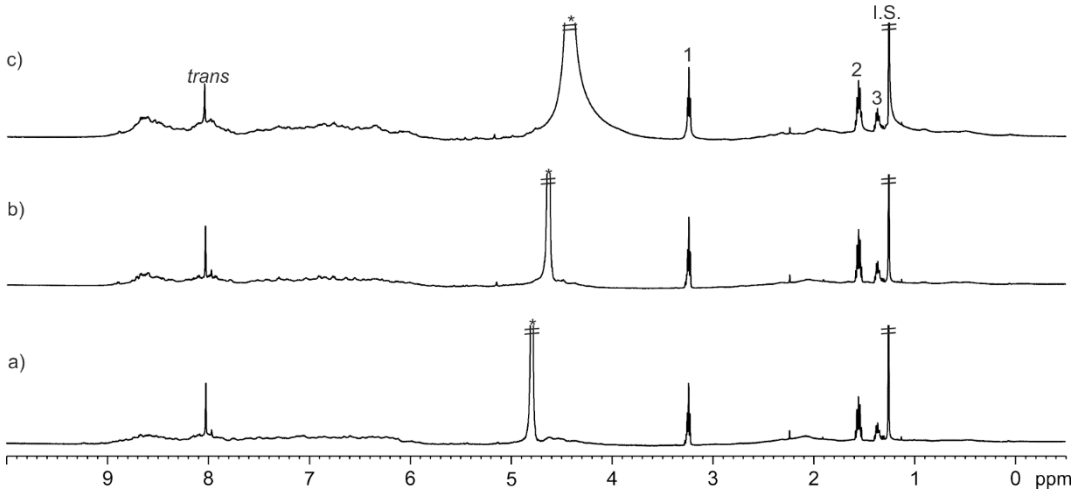

Figure S60. VT ^{1}H NMR (500 MHz with cryoprobe, D_2O) spectra of **2**$^{4+}$ with *ca*. 1 equiv. of **9**: a) 298; b) 313 and c) 333 K. See Figure S49 for proton assignment. *tert*-Butanol (I.S.). *Residual solvent peak.

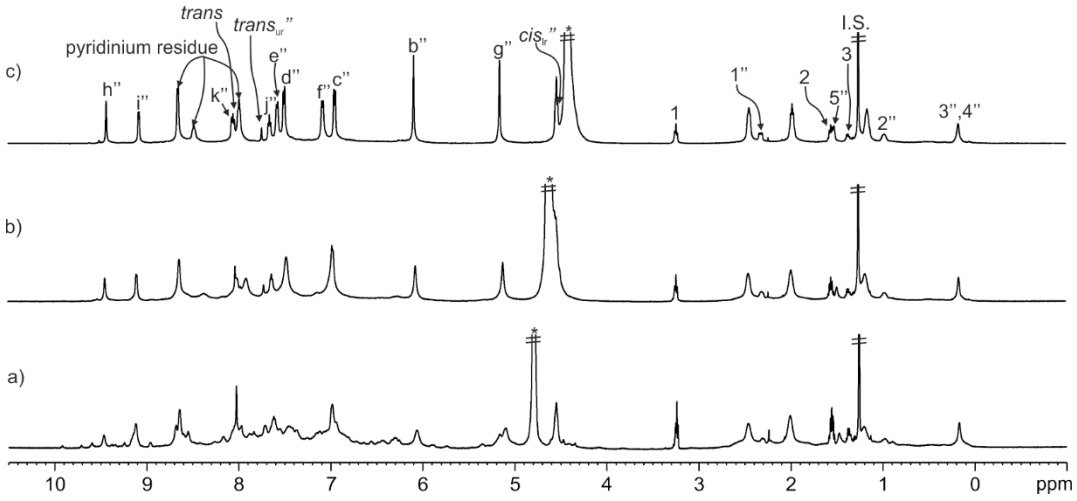

Figure S61. VT ^{1}H NMR (500 MHz with cryoprobe, D_2O) spectra of $\mathbf{2}^{4+}$ with *ca*. 1 equiv. of **9** upon the addition of Pd(II): a) 298; b) 313 and c) 333 K. Doubly primed labels correspond to proton signals of *trans*,*cis*-**9**⊂[**2**•Pd]$^{6+}$. The *trans,cis*-**9**⊂[**2**•Pd]$^{6+}$ cage complex was assembled in 60% extent. See Scheme S2 and Figure S68 for proton assignments. *tert*-Butanol (I.S.). *Residual solvent peak.

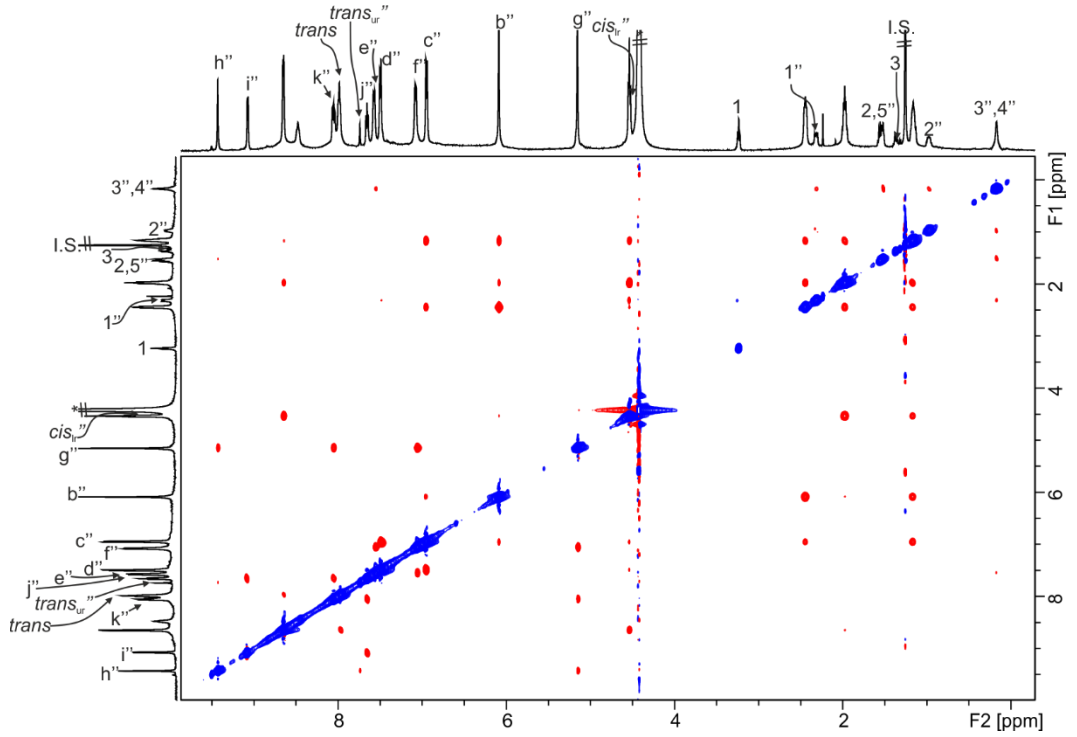

Figure S62. ^{1}H-^{1}H ROESY NMR (500 MHz with cryoprobe, D_2O, 333 K, spin lock = 0.3 s) spectrum of [**2**•Pd]$^{6+}$ with *ca.* 1 equiv. of **9**. See Figure S68 for proton assignment. *Residual solvent peak.

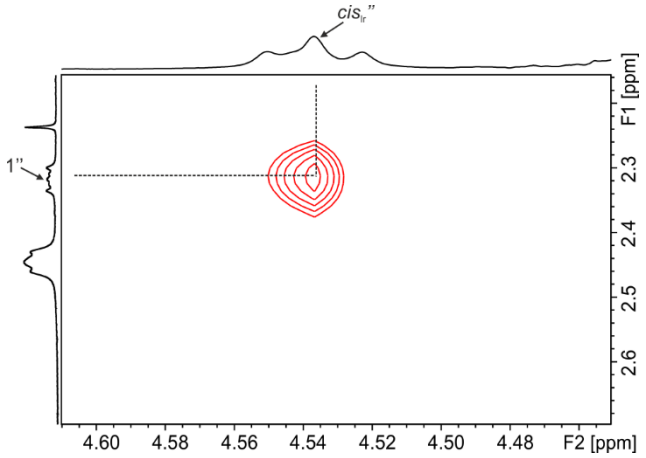

Figure S63. Selected region of the ^{1}H-^{1}H ROESY NMR (500 MHz with cryoprobe, D_2O, 333 K, spin lock = 0.3 s) spectrum of [**2**•Pd]$^{6+}$ with *ca.* 1 equiv. of **9**. The ROESY cross-peak between 1'' and the signal at 4.52 ppm is highlighted. The observed cross-peak confirms that one of the formamide groups of bound **9** adopts a *cis*-conformation. See Figure S68 for proton assignment.

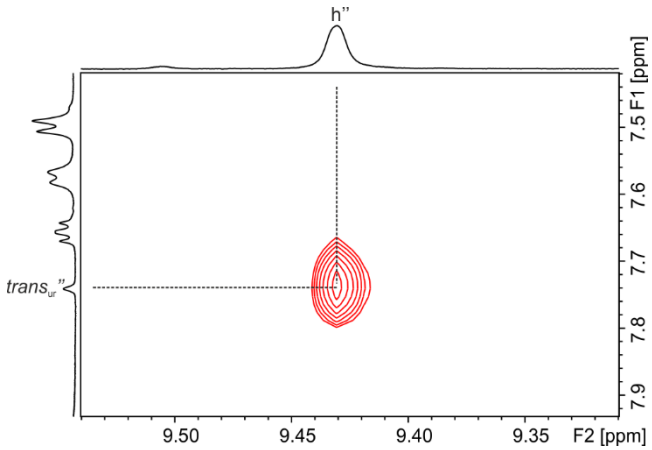

Figure S64. Selected region of the ^{1}H-^{1}H ROESY NMR (500 MHz with cryoprobe, D_2O, 333 K, spin lock = 0.3 s) spectrum of [**2**•Pd]$^{6+}$ with *ca.* 1 equiv. of **9**. The ROESY cross-peak between h'' and *trans*$_{ur}$'' is highlighted. The observed cross-peak indicates that one of the formamide groups of bound *trans*,*cis*-**9** is located in the binding site defined by the inwardly-directed *α*-pyridyl protons. See Scheme S2 and Figure S68 for proton assignments.

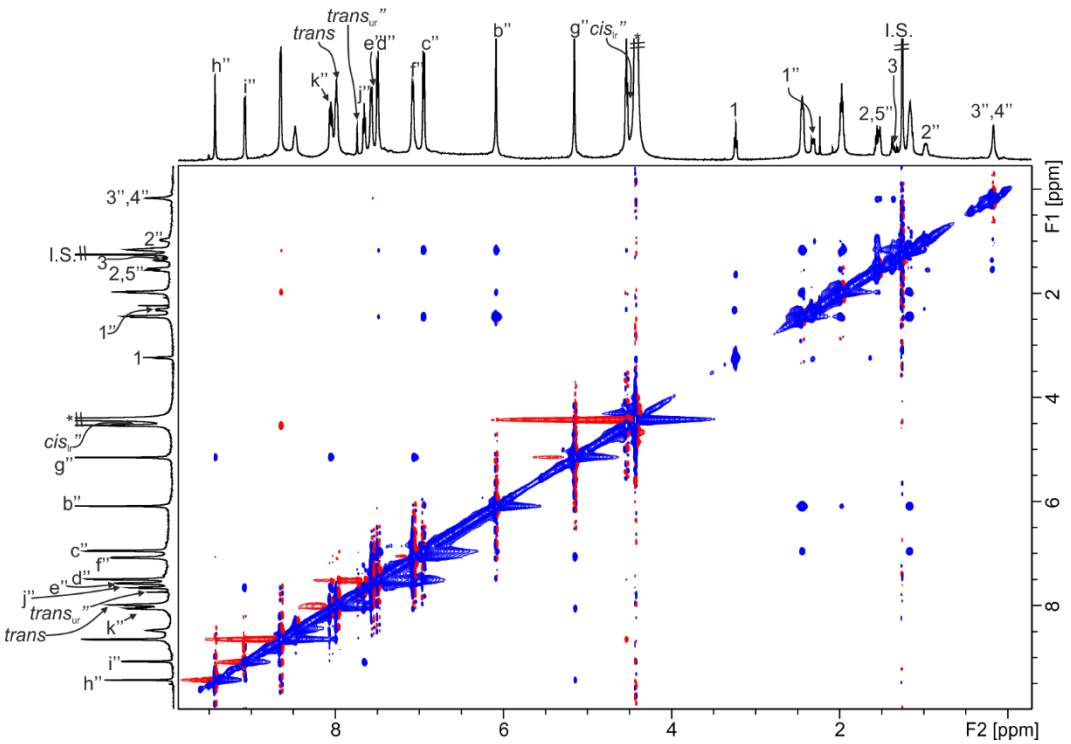

Figure S65. ^{1}H-^{1}H EXSY NMR (500 MHz with cryoprobe, D_2O, 333 K, mixing time = 0.3 s) spectrum of [**2**•Pd]$^{6+}$ with *ca.* 1 equiv. of **9**. See Figure S49 and Figure S68 for proton assignments. *Residual solvent peak.

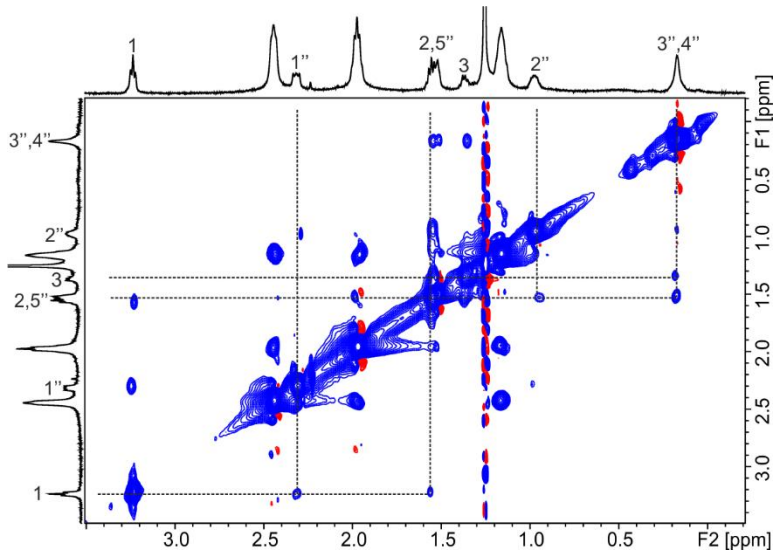

Figure S66. Selected region of the ^{1}H-^{1}H EXSY NMR (500 MHz with cryoprobe, D_2O, 333 K, mixing time = 0.3 s) spectrum of [**2**•Pd]$^{6+}$ with *ca.* 1 equiv. of **9**. See Figure S49 and Figure S68 for proton assignments.

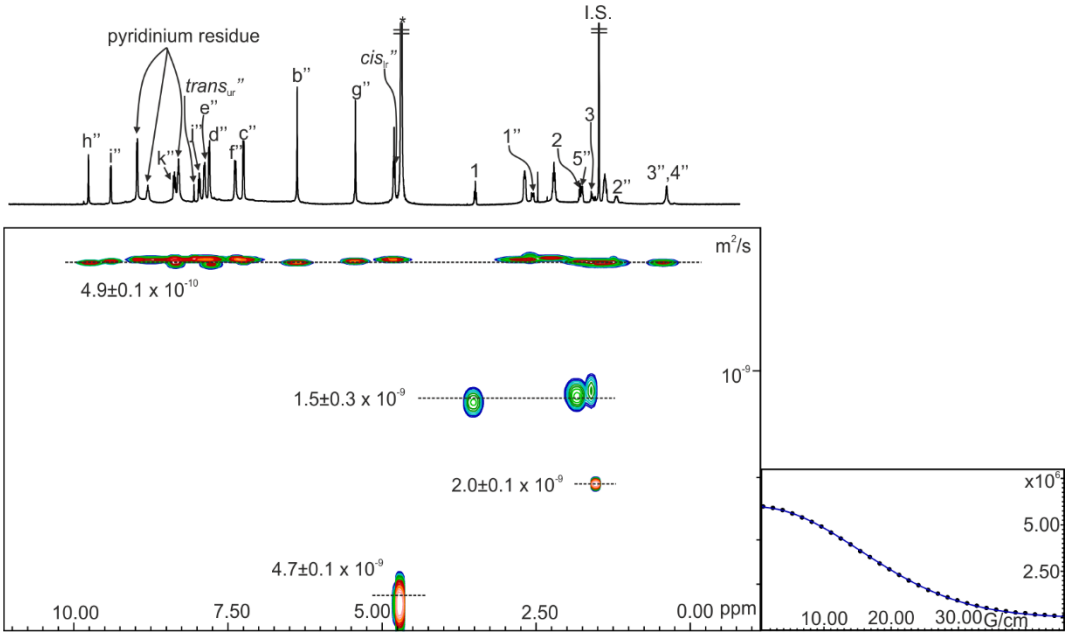

Figure S67. left) ^{1}H pseudo 2D DOSY (500 MHz with cryoprobe, D_2O, 333 K, D20 = 0.20 s; P30 = 0.60 ms) of [**2**•Pd]$^{6+}$ with *ca.* 1 equiv. of **9**. right) Fit of the decay of the signal b'' to a mono-exponential function using Dynamics Center from Bruker. Doubly primed labels correspond to proton signals of *trans*,*cis*-**9**⊂[**2**•Pd]$^{6+}$. See Scheme S2, Figure S49 and Figure S68 for proton assignments. Errors are indicated as standard deviations. *tert*-Butanol (I.S.). *Residual solvent peak.

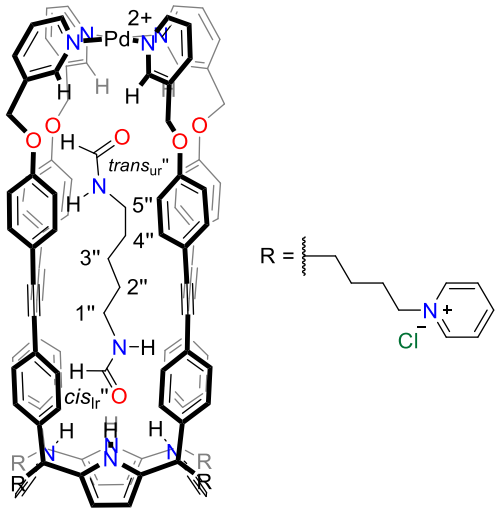

Figure S68. Line-drawing structure of the *trans*,*cis*-**9**⊂[**2**•Pd]$^{6+}$ cage complex.

Table S6. Experimental chemical shifts of free (δ_{free}) and bound (δ_{bound}) *bis*-formamide **9** and complexation-induced shifts ($\Delta\delta$).

Signal	δ_{free} (ppm)	Signal	δ_{bound} (ppm)	$\Delta\delta$ (ppm)
trans	8.04	*trans*$_{ur}$''	7.74	-0.30
cis	7.99	*cis*$_{lr}$''	4.52	-3.47
1	3.24	1''	2.31	-0.93
2	1.56	2''	0.98	-0.58
3	1.37	3''	0.17	-1.20
-	-	4''	0.17	-1.39
-	-	5''	1.53	-1.71

Mono-formamide **10**

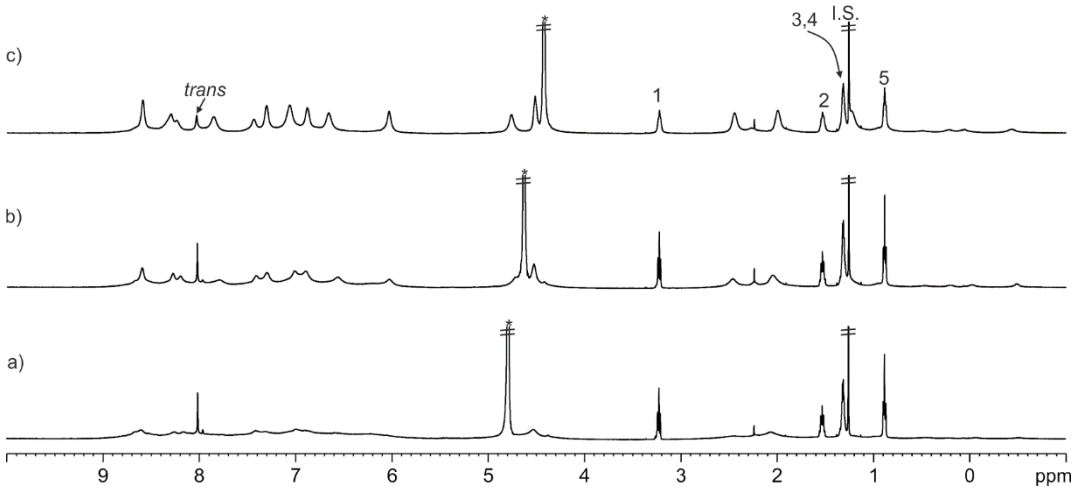

Figure S69. VT ^{1}H NMR (500 MHz with cryoprobe, D_2O) spectra of $\mathbf{2}^{4+}$ with *ca.* 1 equiv. of **10**: a) 298; b) 313 and c) 333 K. See Figure S49 for proton assignment. *tert*-Butanol (I.S.). *Residual solvent peak.

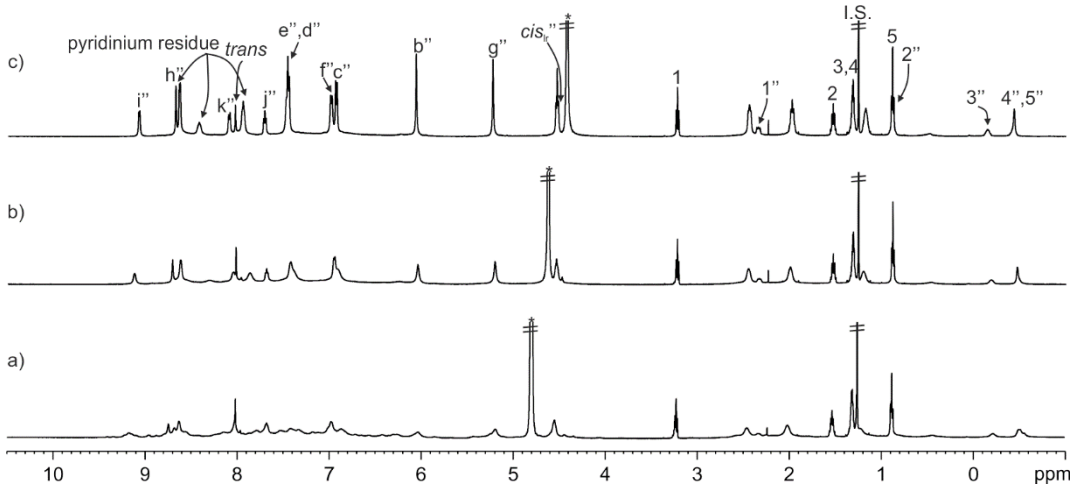

Figure S70. VT ^{1}H NMR (500 MHz with cryoprobe, D_2O) spectra of $\mathbf{2}^{4+}$ with *ca.* 1 equiv. of **10** upon the addition of *ca.* 1 equiv. of Pd(II): a) 298; b) 313 and 333 K. Doubly primed labels correspond to proton signals of *cis*-**10**⊂[**2**•Pd]$^{6+}$. The *cis*-**10**⊂[**2**•Pd]$^{6+}$ cage complex was assembled in 60% extent. See Scheme S2 and Figure S79 for proton assignments. *tert*-butanol (I.S.). *Residual solvent peak.

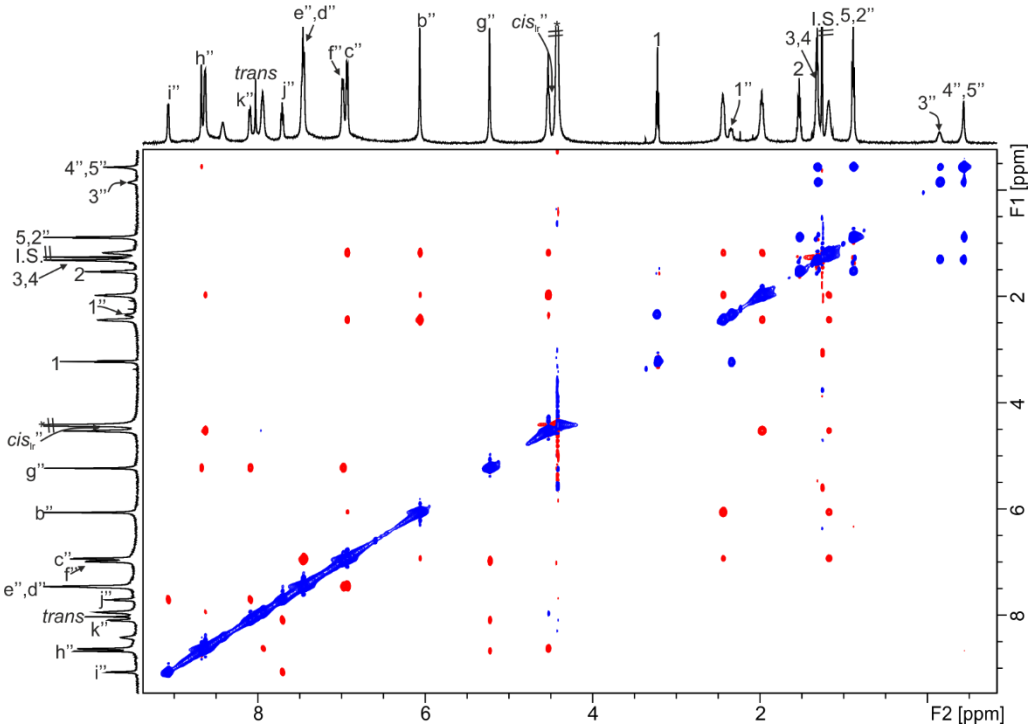

Figure S71. ^{1}H-^{1}H ROESY NMR (500 MHz with cryoprobe, D_2O, 333 K, spin lock = 0.3 s) spectrum of [**2**•Pd]$^{6+}$ with *ca.* 1 equiv. of **10**. See Figure S79 for proton assignment. *Residual solvent peak.

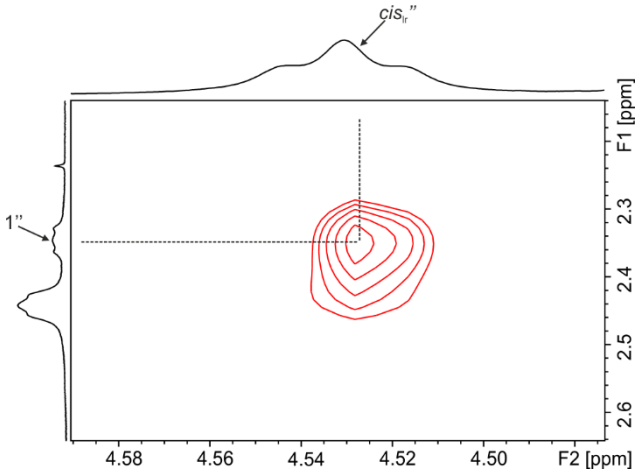

Figure S72. Selected region of the ^{1}H-^{1}H ROESY NMR (500 MHz with cryoprobe, D_2O, 333 K, spin lock = 0.3 s) spectrum of [**2**•Pd]$^{6+}$ with *ca.* 1 equiv. of **10**. The ROESY cross-peak between 1'' and the signal at 4.52 ppm is highlighted. The observed cross-peak confirms that the formamide group of bound **10** adopts a *cis*-conformation. See Figure S79 for proton assignment.

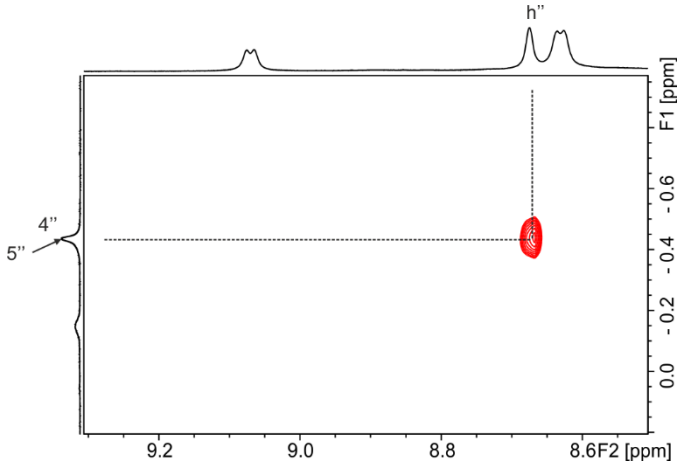

Figure S73. Selected region of the ^{1}H-^{1}H ROESY NMR (500 MHz with cryoprobe, D_2O, 333 K, spin lock = 0.3 s) spectrum of [**2**•Pd]$^{6+}$ with *ca.* 1 equiv. of **10**. The ROESY cross-peak between h'' and 5'' is highlighted. The observed cross-peak indicates that the methyl group of bound *cis*-**10** is located in the binding site defined by the inwardly-directed *α*-pyridyl protons. See Scheme S2 and Figure S79 for proton assignments.

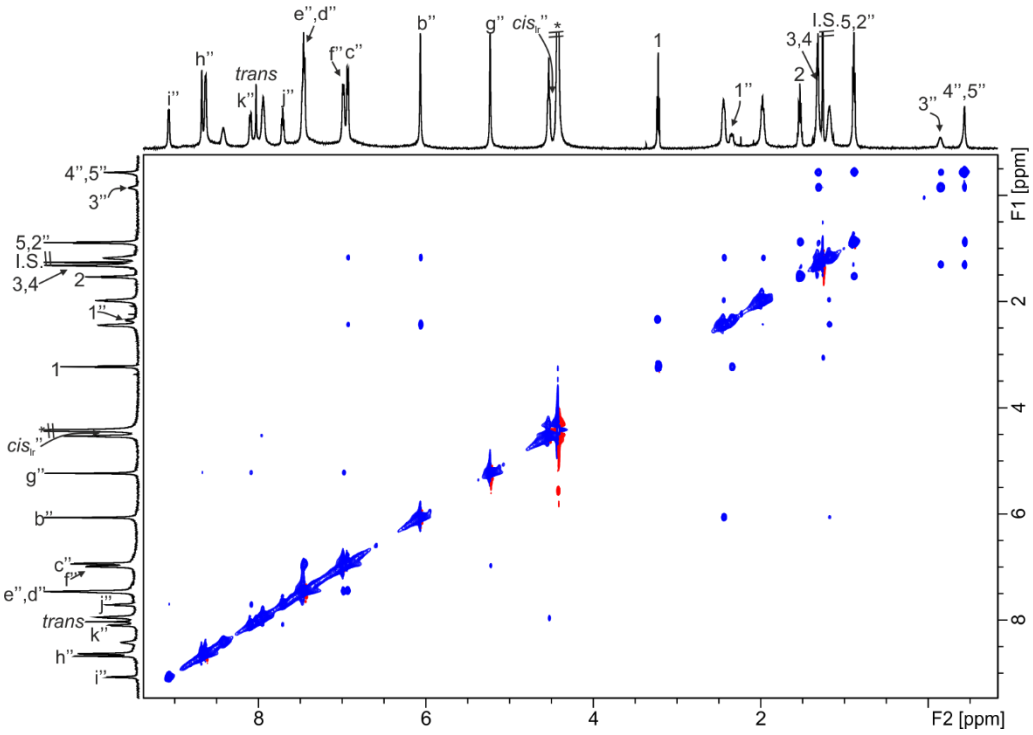

Figure S74. ^{1}H-^{1}H EXSY NMR (500 MHz with cryoprobe, D_2O, 333 K, mixing time = 0.3 s) spectrum of [**2**•Pd]$^{6+}$ with *ca.* 1 equiv. of **10**. See Figure S49 and Figure S79 for proton assignments. *Residual solvent peak.

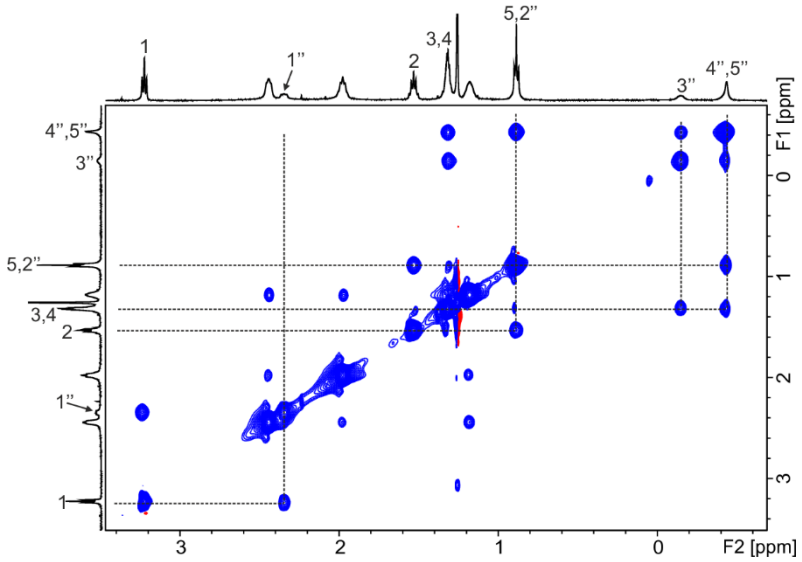

Figure S75. Selected region of the ^{1}H-^{1}H EXSY NMR (500 MHz with cryoprobe, D_2O, 333 K, mixing time = 0.3 s) spectrum of [**2**•Pd]$^{6+}$ with *ca.* 1 equiv. of **10**. See Figure S49 and Figure S79 for proton assignments.

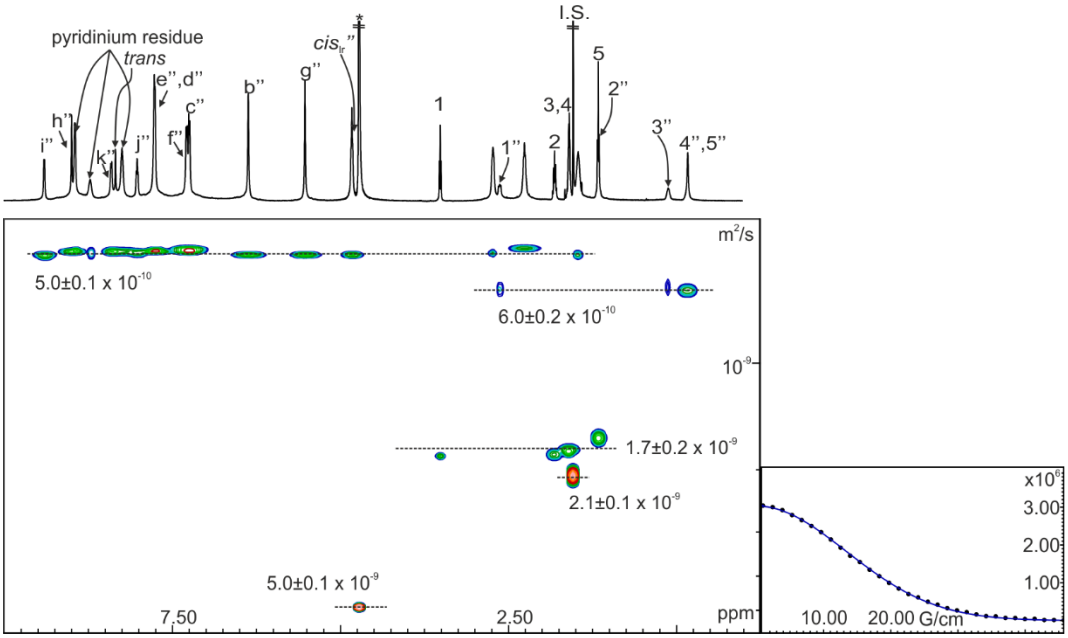

Figure S76. left) ^{1}H pseudo 2D DOSY (500 MHz with cryoprobe, D_2O, 333 K, D20 = 0.20 s; P30 = 0.60 ms) of [**2**•Pd]$^{6+}$ with *ca.* 2 equiv. of **10**. right) Fit of the decay of the signal b'' to a mono-exponential function using Dynamics Center from Bruker. Doubly primed labels correspond to proton signals of *cis*-**10**⊂[**2**•Pd]$^{6+}$. See Scheme S2, Figure S49 and Figure S79 for proton assignments. Errors are indicated as standard deviations. *tert*-Butanol (I.S.). *Residual solvent peak.

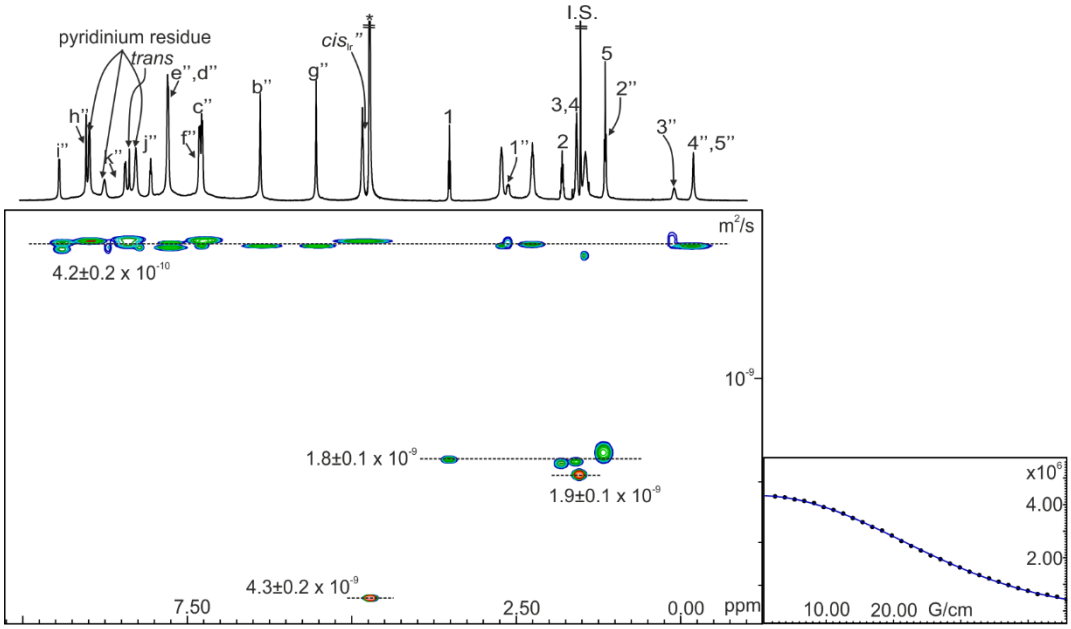

Figure S77. left) ^{1}H pseudo 2D DOSY (500 MHz with cryoprobe, D_2O, 333 K, D20 = 0.01 s; P30 = 3.50 ms) of [**2**•Pd]$^{6+}$ with *ca.* 2 equiv. of **10**. right) Fit of the decay of the signal b'' to a mono-exponential function using Dynamics Center from Bruker. Doubly primed labels correspond to proton signals of *cis*-**10**⊂[**2**•Pd]$^{6+}$. See Scheme S2, Figure S49 and Figure S79 for proton assignments. Errors are indicated as standard deviations. *tert*-Butanol (I.S.). *Residual solvent peak.

The diffusion constant value of bound *cis*-**10** differed from those of the [**2**•Pd]$^{6+}$ cage and the free guest **10** in the DOSY experiment with a diffusion time t_d ~ 200 ms (Figure S76). On the contrary, the diffusion constant of bound *cis*-**10** coincided with that of the [**2**•Pd]$^{6+}$ cage when the diffusion time was significantly reduced, t_d ~ 10 ms (Figure S77). The result obtained with t_d ~ 200 ms indicates that magnetization transfer between bound and free guest molecules occurs during the diffusion time (t_d) in a significant extent.[5]

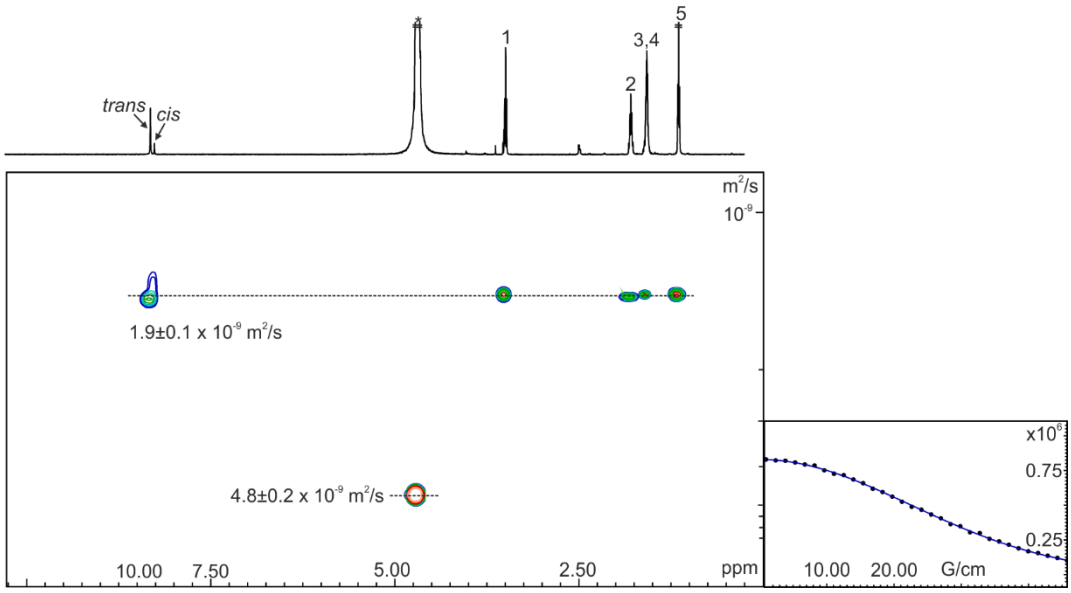

Figure S78. left) ^{1}H pseudo 2D DOSY (500 MHz with cryoprobe, D_2O, 333 K, D20 = 0.20 s; P30 = 0.30 ms) of **10**. right) Fit of the decay of the signal 3 to a mono-exponential function using Dynamics Center from Bruker. See Figure S49 for proton assignment. Errors are indicated as standard deviations. *Residual solvent peak.

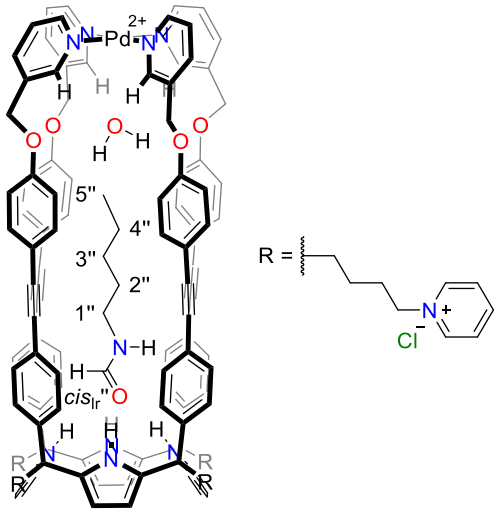

Figure S79. Line-drawing structure of the putative [*cis*-**10**•H_2O]⊂[**2**•Pd]$^{6+}$ cage complex.

Table S7. Experimental chemical shifts of free (δ_{free}) and bound (δ_{bound}) *mono*-formamide **10** and complexation-induced shifts ($\Delta\delta$).

Signal	δ_{free} (ppm)	Signal	δ_{bound} (ppm)	$\Delta\delta$ (ppm)
trans	8.03	-	-	-
cis	7.98	cis_{lr}''	4.52	-3.46
1	3.22	1''	2.35	-0.87
2	1.53	2''	0.88	-0.65
3	1.32	3''	-0.14	-1.46
4	1.32	4''	-0.43	-1.75
5	0.88	5''	-0.43	-1.31

5.4 Chemical shifts of the *α*-pyridyl protons in the self-assembled Pd(II)-cage complexes

Table S8. Chemical shifts (δ) of the *α*-pyridyl proton signals in the assembled [**2**•Pd]$^{6+}$ cage complexes in D_2O solution at 333 K.

Cage complex	δ of signal h'' (ppm)	δ of signal i'' (ppm)
5⊂[**2**•Pd]$^{6+}$	9.09	9.05
6⊂[**2**•Pd]$^{6+}$	9.44	9.05
cis,*cis*-**8**⊂[**2**•Pd]$^{6+}$	9.58	9.07
trans,*cis*-**9**⊂[**2**•Pd]$^{6+}$	9.43	9.08
cis-**10**⊂[**2**•Pd]$^{6+}$	8.68	9.07

The chemical shifts of the *α*-pyridyl proton signals of tetra-pyridinium SAE-C[4]P tetra-pyridyl ligand **2**$^{4+}$, h'' and i'', upon the addition of *ca.* 1 equiv. of Pd(II) to the equimolar D_2O solution of **2**$^{4+}$ and guest (**5**,**6** and **8**-**10**) are in agreement with the formation of pyridyl-Pd(II) coordination bonds.[3]

6. Displacement of the included guest in selected cage complexes using the *bis*-*N*-oxide 5 as a competitive binding guest

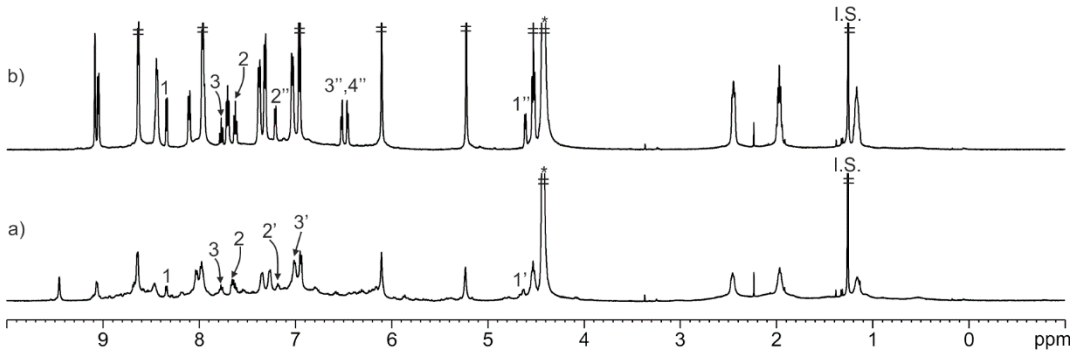

Figure S80. ^{1}H NMR (500 MHz with cryoprobe, D_2O, 333 K) spectra of: a) [**2**•Pd]$^{6+}$ with *ca.* 1 equiv. of **6** and b) addition of *ca.* 1 equiv. of **5** to a). Primed labels correspond to proton signals of **6**⊂[**2**•Pd]$^{6+}$. Doubly primed labels correspond to proton signals of **5**⊂[**2**•Pd]$^{6+}$. See Figure S33, Figure S42 and Figure S46 for proton assignments. *tert*-Butanol (I.S.). *Residual solvent peak.

The **6**⊂[**2**•Pd]$^{6+}$ cage complex was assembled in 30% extent (Figure S80a). The addition of *bis*-*N*-oxide **5** to the D_2O solution of **6**⊂[**2**•Pd]$^{6+}$ produced the rapid formation of the **5**⊂[**2**•Pd]$^{6+}$ cage complex in 60% extent. Concomitantly, the bound guest **6** was released to the bulk solution (Figure S80b).

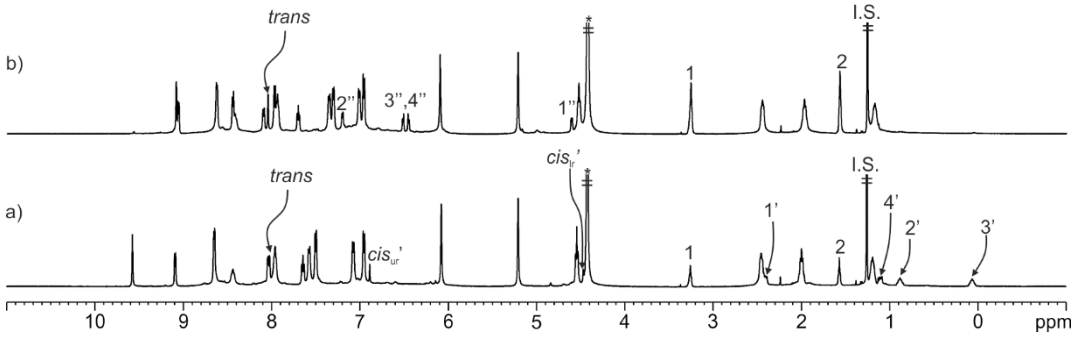

Figure S81. ^{1}H NMR (500 MHz with cryoprobe, D_2O, 333 K) spectra of: a) [**2**•Pd]$^{6+}$ with *ca.* 1 equiv. of **8** and b) addition of *ca.* 1 equiv. of **5** to a). Primed labels correspond to proton signals of *cis*,*cis*-**8**⊂[**2**•Pd]$^{6+}$. Doubly primed labels correspond to proton signals of **5**⊂[**2**•Pd]$^{6+}$. See Figure S42, Figure S49 and Figure S59 for proton assignments. *tert*-Butanol (I.S.). *Residual solvent peak.

The *cis,cis*-**8**⊂[**2**•Pd]$^{6+}$ cage complex was assembled in 60% extent (Figure S81a). The addition of *bis*-*N*-oxide **5** to the D_2O solution of *cis,cis*-**8**⊂[**2**•Pd]$^{6+}$ produced the rapid formation of the **5**⊂[**2**•Pd]$^{6+}$ cage complex in 60% extent. Concomitantly, the bound guest **8** was released to the bulk solution (Figure S81b).

7. Addition of $(CD_3)_2SO$ to the D_2O solutions of ligand 2, ligand 2 with *bis*-formamide 8 and selected Pd(II)-cage complexes

Tetra-pyridinium SAE-C[4]P tetra-pyridyl ligand $\mathbf{2}^{4+}$

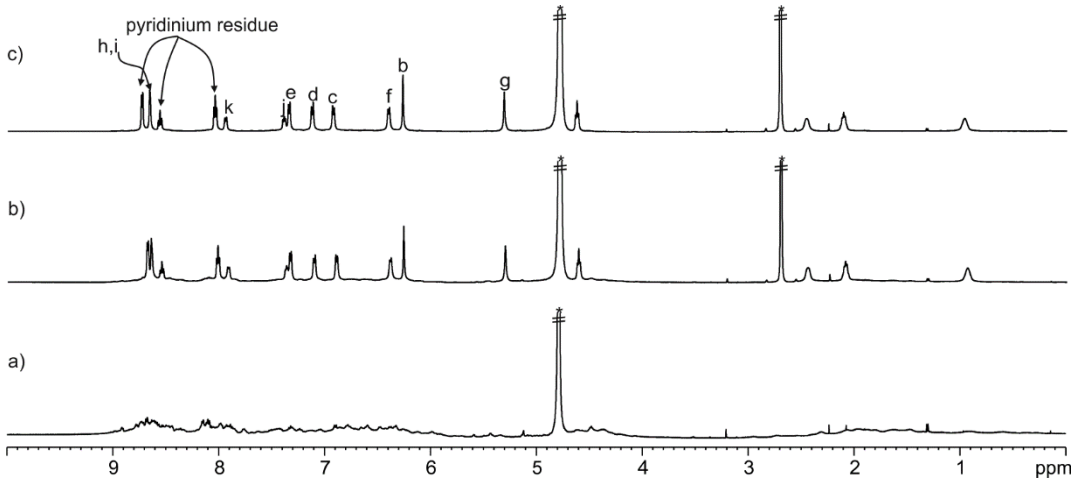

Figure S82. ^{1}H NMR (500 MHz with cryoprobe, D_2O, 298 K) spectra of $\mathbf{2}^{4+}$ upon addition of: a) 0; b) *ca.* 10 and c) *ca.* 20% vol. $(CD_3)_2SO$. See Scheme S2 for proton assignment. *Residual solvent peaks.

Tetra-pyridinium SAE-C[4]P tetra-pyridyl ligand $\mathbf{2}^{4+}$ in 1:9 $(CD_3)_2SO/D_2O$ solution, followed by the addition of Pd(II)

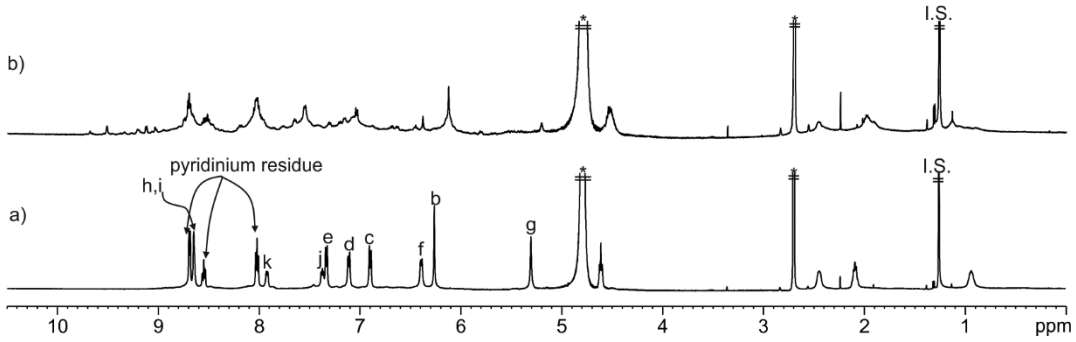

Figure S83. ^{1}H NMR (500 MHz with cryoprobe, 1:9 $(CD_3)_2SO/D_2O$, 298 K) spectra of: a) $\mathbf{2}^{4+}$ and b) $\mathbf{2}^{4+}$ with *ca*. 1 equiv. of $Pd(NO_3)_2$. See Scheme S2 for proton assignment. *tert*-Butanol (I.S.). *Residual solvent peaks.

Tetra-pyridinium SAE-C[4]P tetra-pyridyl ligand **2**$^{4+}$ with *bis*-formamide **8**

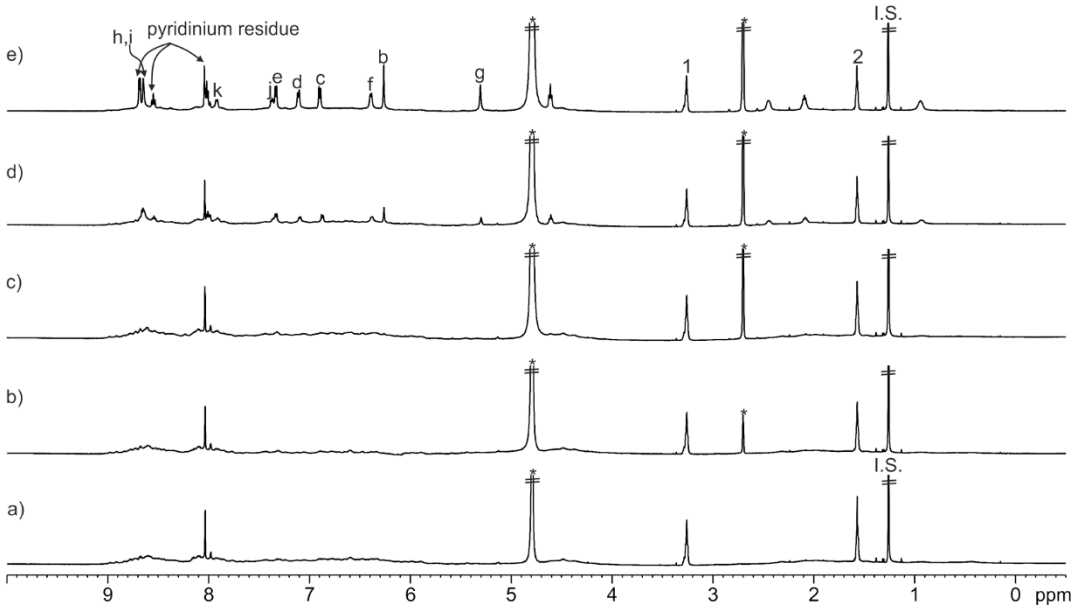

Figure S84. ^{1}H NMR (500 MHz with cryoprobe, D_2O, 298 K) spectra of **2**$^{4+}$ with *ca.* 1 equiv. of **8** upon addition of: a) 0; b) *ca.* 1; c) *ca.* 2; d) *ca.* 5 and e) *ca.* 10% vol. $(CD_3)_2SO$. See Scheme S2 and Figure S49 for proton assignments. *tert*-Butanol (I.S.). *Residual solvent peaks.

5⊂[**2**•Pd]$^{6+}$ cage complex

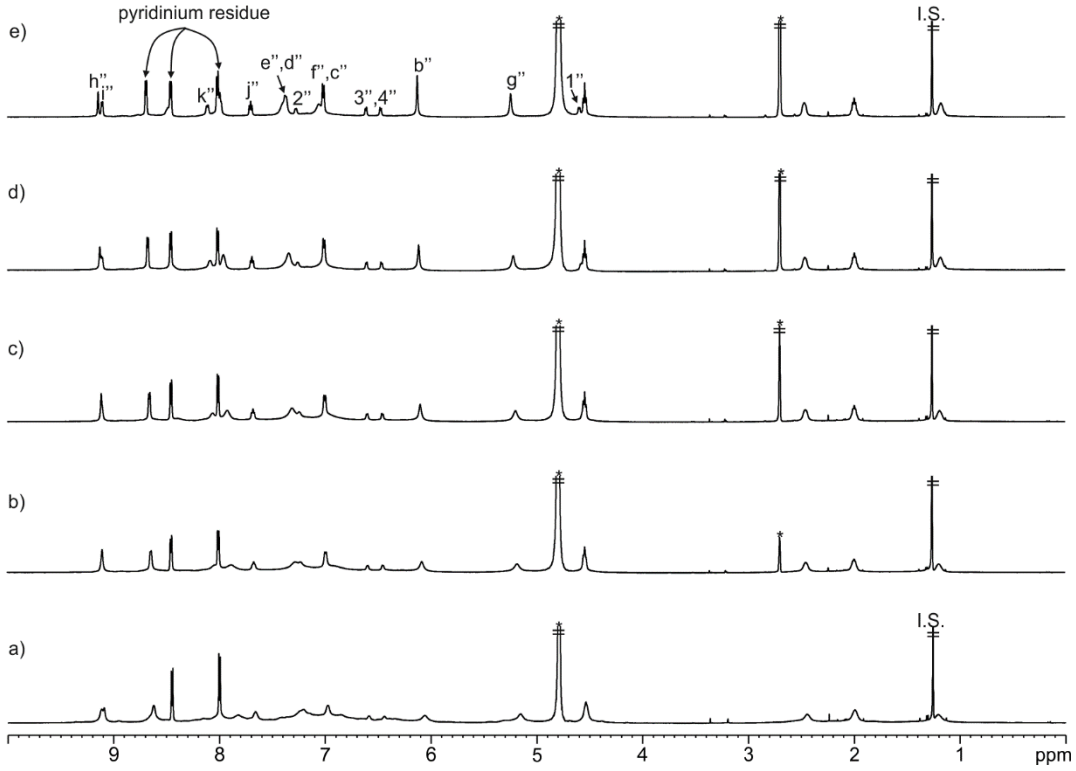

Figure S85. ^{1}H NMR (500 MHz with cryoprobe, D_2O, 298 K) spectra of **5**⊂[**2**•Pd]$^{6+}$ upon addition of: a) 0; b) *ca.* 1; c) *ca.* 2; d) *ca.* 5 and e) *ca.* 10% vol. $(CD_3)_2SO$. Doubly primed labels correspond to proton signals of **5**⊂[**2**•Pd]$^{6+}$. See Scheme S2 and Figure S42 for proton assignments. *tert*-Butanol (I.S.). *Residual solvent peaks.

cis,cis-**8**⊂[**2**•Pd]$^{6+}$ cage complex

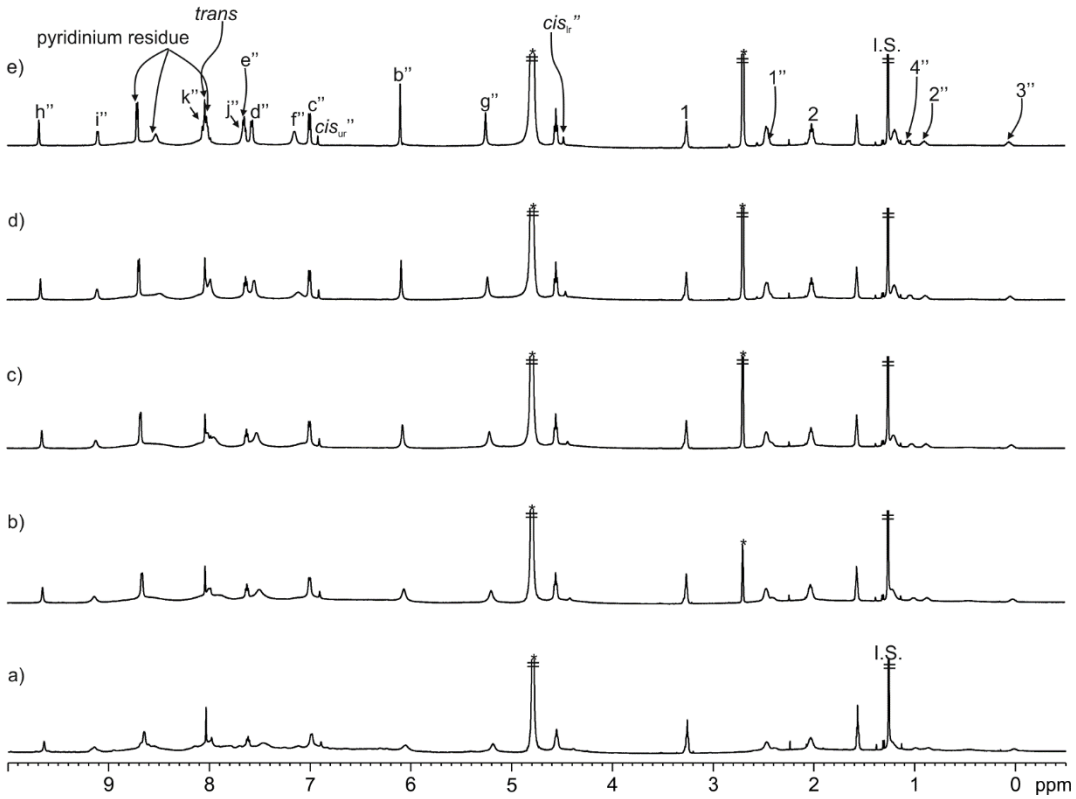

Figure S86. ^{1}H NMR (500 MHz with cryoprobe, D_2O, 298 K) spectra of *cis,cis*-**8**⊂[**2**•Pd]$^{6+}$ upon addition of: a) 0; b) *ca.* 1; c) *ca.* 2; d) *ca.* 5 and e) *ca.* 10% vol. $(CD_3)_2SO$. Doubly primed labels correspond to proton signals of *cis,cis*-**8**⊂[**2**•Pd]$^{6+}$. See Scheme S2, Figure S49 and Figure S59 for proton assignments. *tert*-Butanol (I.S.). *Residual solvent peaks.

cis-**10**⊂[**2**•Pd]$^{6+}$ cage complex

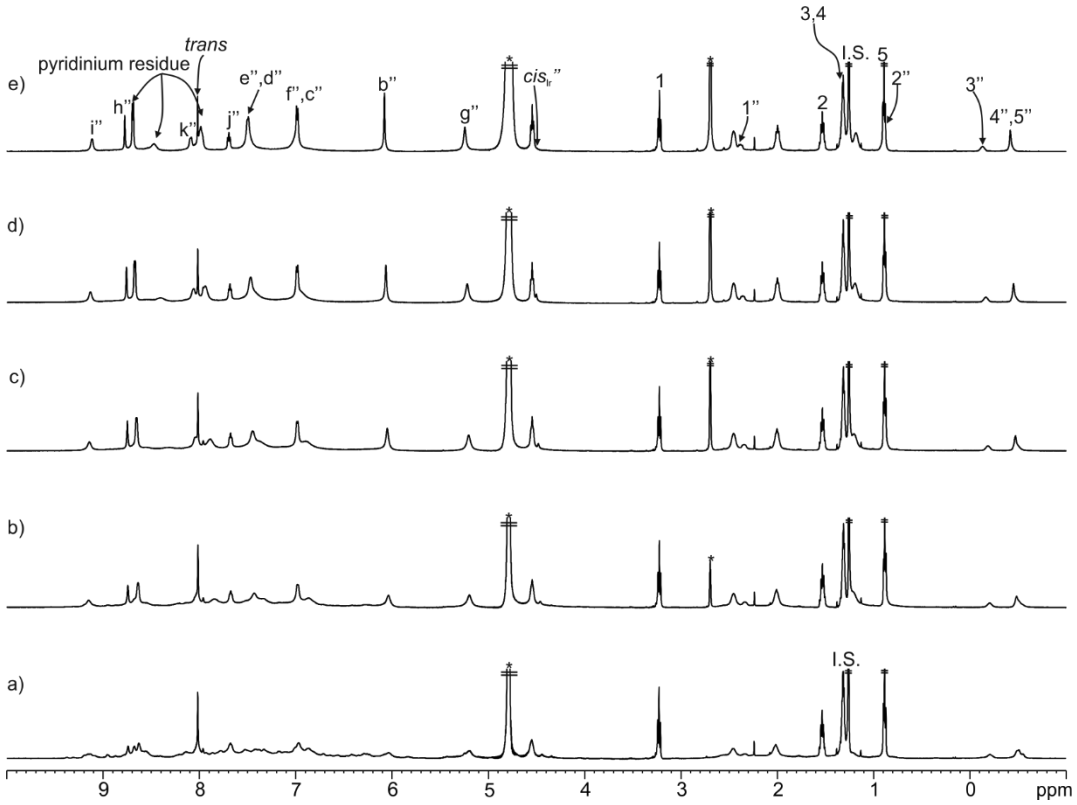

Figure S87. ^{1}H NMR (500 MHz with cryoprobe, D_2O, 298 K) spectra of *cis*-**10**⊂[**2**•Pd]$^{6+}$ upon addition of: a) 0; b) *ca.* 1; c) *ca.* 2; d) *ca.* 5 and e) *ca.* 10% vol. $(CD_3)_2SO$. Doubly primed labels correspond to proton signals of *cis*-**10**⊂[**2**•Pd]$^{6+}$. See Scheme S2, Figure S49 and Figure S79 for proton assignments. *tert*-Butanol (I.S.). *Residual solvent peaks.

The addition of *ca.* 10% of $(CD_3)_2SO$ to the millimolar D_2O solutions of the ligand **2**$^{4+}$ and the Pd(II)-cage complexes, **5**⊂[**2**•Pd]$^{6+}$, *cis*,*cis*-**8**⊂[**2**•Pd]$^{6+}$ and *cis*-**10**⊂[**2**•Pd]$^{6+}$, provoked the sharpening of the proton signals in the NMR spectra at 298 K. These results, together with those obtained using variable-temperature (VT) ^{1}H NMR experiments, indicated that the ligand **2**$^{4+}$, as well as the Pd(II)-cage complexes, form ill-defined aggregates in water solution at r.t.

8. Energy-minimized structures of the Pd(II)-cage complexes

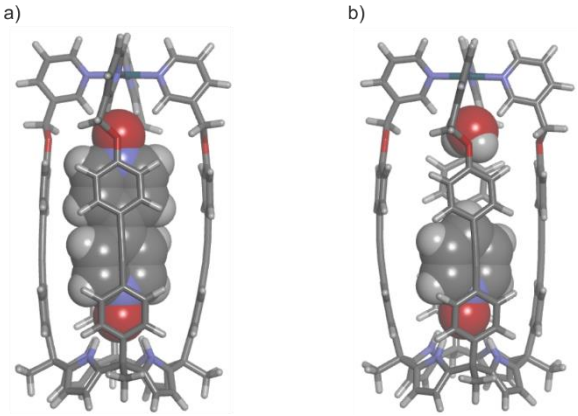

Figure S88. Energy minimized structures (MM3) of simplified Pd(II)-cage complexes: a) **5**⊂[**2**•Pd]$^{6+}$ and b) [**6**•H_2O]⊂[**2**•Pd]$^{6+}$. The Pd(II)-cages are depicted in stick representation and the bound guests are shown as CPK models. Water-solubilizing groups were pruned to methyl groups to simplify the calculations.

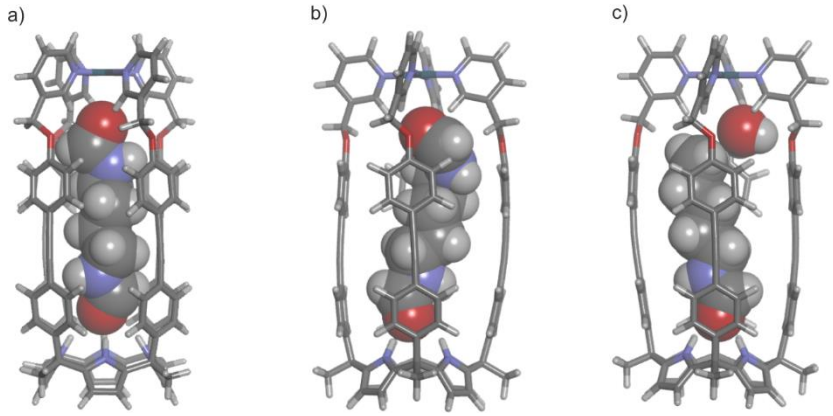

Figure S89. Energy minimized structures (MM3) of simplified Pd(II)-cage complexes: a) *cis,cis*-**8**⊂[**2**•Pd]$^{6+}$; b) *trans,cis*-**9**⊂[**2**•Pd]$^{6+}$ and c) [*cis*-**10**•H_2O]⊂[**2**•Pd]$^{6+}$. The Pd(II)-cages are depicted in stick representation and the bound guests are shown as CPK models. Water-solubilizing groups were pruned to methyl groups to simplify the calculations.

9. X-ray crystal structures

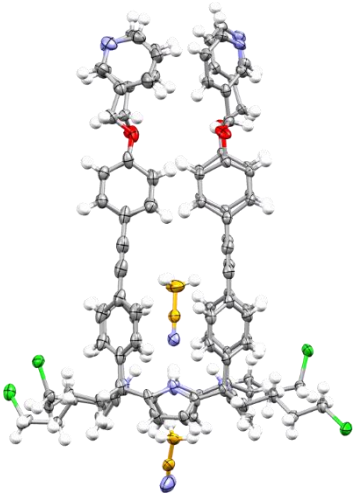

Figure S90. X-ray crystal structure of tetra-pyridyl ligand **1b**. The structure is shown in ORTEP view with thermal ellipsoids set at 50% probability. Hydrogen atoms are shown as fixed-size spheres of 0.3 Å radius. CCDC 2093909.

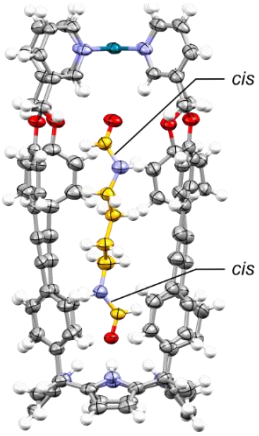

Figure S91. X-ray crystal structure of *cis*,*cis*-**8**⊂[**1a**•Pd]$^{2+}$ cage complex. The structure is shown in ORTEP view with thermal ellipsoids set at 50% probability. Hydrogen atoms are shown as fixed-size spheres of 0.3 Å radius. CCDC 2093910.

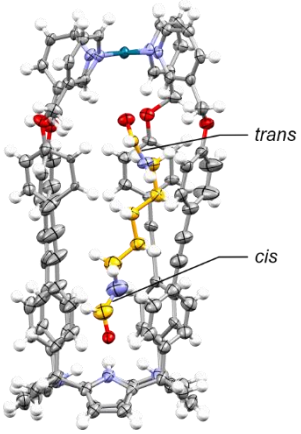

Figure S92. X-ray crystal structure of *trans*,*cis*-**9**⊂[**1a**•Pd]$^{2+}$ cage complex. The structure is shown in ORTEP view with thermal ellipsoids set at 50% probability. Hydrogen atoms are shown as fixed-size spheres of 0.3 Å radius. CCDC 2093911.

10. References

[1] G. R. Fulmer, A. J. M. Miller, N. H. Sherden, H. E. Gottlieb, A. Nudelman, B. M. Stoltz, J. E. Bercaw and K. I. Goldberg, *Organometallics*, 2010, **29**, 2176-2179.

[2] L. Escobar and P. Ballester, *Org. Chem. Front.*, 2019, **6**, 1738-1748.

[3] L. Escobar, D. Villarón, E. C. Escudero-Adán and P. Ballester, *Chem. Commun. (Cambridge, U. K.)*, 2019, **55**, 604-607.

[4] Q. Sun, L. Escobar and P. Ballester, *Angew. Chem., Int. Ed.*, 2021, **60**, 10359-10365.

[5] L. Escobar, Y.-S. Li, Y. Cohen, Y. Yu, J. Rebek Jr and P. Ballester, *Chem.-Eur. J.*, 2020, **26**, 8220-8225.